Constraining spacetime torsion with the Moon and Mercury

Riccardo March
Istituto per le Applicazioni del Calcolo, CNR, Via dei Taurini 19, 00185 Roma, Italy,
and INFN - Laboratori Nazionali di Frascati (LNF), via E. Fermi 40 Frascati, 00044 Roma, Italy.
E-mail: r.march@iac.cnr.it

Giovanni Bellettini
Dipartimento di Matematica, Università di Roma "Tor Vergata",
via della Ricerca Scientifica 1, 00133 Roma, Italy,
and INFN - Laboratori Nazionali di Frascati (LNF), via E. Fermi 40 Frascati, 00044 Roma, Italy.
E-mail: Giovanni.Bellettini@lnf.infn.it

Roberto Tauraso
Dipartimento di Matematica, Università di Roma "Tor Vergata",
via della Ricerca Scientifica 1, 00133 Roma, Italy,
and INFN - Laboratori Nazionali di Frascati (LNF), via E. Fermi 40 Frascati, 00044 Roma, Italy.
E-mail: tauraso@mat.uniroma2.it

Simone Dell'Agnello
INFN - Laboratori Nazionali di Frascati (LNF), via E. Fermi 40 Frascati, 00044 Roma, Italy.
E-mail: Simone.Dellagnello@lnf.infn.it

Abstract

We report a search for new gravitational physics phenomena based on Riemann-Cartan theory of General Relativity including spacetime torsion. Starting from the parametrized torsion framework of Mao, Tegmark, Guth and Cabi, we analyze the motion of test bodies in the presence of torsion, and in particular we compute the corrections to the perihelion advance and to the orbital geodetic precession of a satellite. We consider the motion of a test body in a spherically symmetric field, and the motion of a satellite in the gravitational field of the Sun and the Earth. We describe the torsion field by means of three parameters, and we make use of the autoparallel trajectories, which in general differ from geodesics when torsion is present. We derive the specific approximate expression of the corresponding system of ordinary differential equations, which are then solved with methods of Celestial Mechanics. We calculate the secular variations of the longitudes of the node and of the pericenter of the satellite. The computed secular variations show how the corrections to the perihelion advance and to the orbital de Sitter effect depend on the torsion parameters. All computations are performed under the assumptions of weak field and slow motion. To test our predictions, we use the measurements of the Moon's geodetic precession from lunar laser ranging data, and the measurements of Mercury's perihelion advance from planetary radar ranging data. These measurements are then used to constrain suitable linear combinations of the torsion parameters.

Keywords: Riemann-Cartan spacetime, torsion, autoparallel trajectories, geodetic precession, perihelion advance, lunar laser ranging, planetary radar ranging.

PACS: 04.50.Kd, 04.80.Cc

1 Introduction

Einstein's theory of General Relativity (GR) successfully describes gravitational physics in the solar system. Its predictions have passed a wide variey of precision experimental tests carried out in weak-field and slow-motion regime with natural bodies and artificial satellites [1], [2]. These tests include the measurement and verification of (quoted in terms of relative experimental uncertainty): Mercury's perihelion advance at 10^{-3} level through planetary radar ranging [3]; the redshift of spectral lines of a hydrogen-maser frequency standard at 10^{-4} level performed with the Gravity Probe A spacecraft [4]; the deflection of light by solar gravity via very-long-baseline (radio) interferometry at 10^{-4} level [5]; the time-delay by gravitational potential using the Viking spacecrafts at Mars [6] and the Cassini mission at Saturn (the latter at 10^{-5} level [7]); the equivalence principle at 10^{-13} level and the geodetic precession at about six parts in 10^{-3} with lunar laser ranging (LLR) of the Apollo and Lunokhod retroreflectors [8]; frame dragging with satellite laser ranging (SLR) of the LAGEOS satellites and with the Gravity Probe B (GPB) mission (the former at 10^{-1} level [9]); the latter is also expected to yield a very accurate measurement of the geodetic precession.
The first three measurements above (perihelion precession, gravitational redshift and light deflection) are the three *classical tests* originally proposed by Einstein to verify his theory. The geodetic precession is a relativistic three-body effect that was predicted [10] by de Sitter in 1916 and observed in 1988 by I.I. Shapiro et al. with an accuracy of 2% using LLR data [11].
In the effort of improving the experimental measurements and of possibly discovering new physics, several extensions and modifications of GR have been developed. One notable attempt is the Parametrized Post-Newtonian (PPN) formalism, whose verification has been the object of continuous and always improving experimental tests. No deviation from GR has been found so far. However, in presence of new physics beyond GR, it is natural to expect and try to measure modifications of the solar system observables described above, which historically marked the transition from newtonian physics to relativistic gravity.
In this paper we treat the modification of GR to include spacetime torsion and motion along autoparallel orbits. Then we use the measured Moon geodetic precession and Mercury's perihelion advance to test our predictions. In a companion paper [12], we show how the constraints on torsion provided by the measurement of the geodetic precession can be used also to constrain spacetime torsion with the frame dragging experiments on LAGEOS satellites.
In the near future, improvements of the limits reported in these two papers may be obtained from the analysis of Mercury radar ranging (MRR) data taken since 1990 [1], from the relentless analysis of more LLR data from more ground stations, from the mm-level range precision provided by the new APOLLO station at Apache Point, USA [13] (operational since 2007) and from the release of the geodetic precession measurement by the GPB Collaboration. In the mid-term we expect a substantial advance from LLR with the deployment of 2^{nd} generation laser retroreflector payloads with robotic soft-landings on the Moon, like the missions of the International Lunar Network (ILN), or similar geophysical

network, and like JAXA's Selene-2. We also expect that in the long term, more stringent limits can be set with the approved BepiColombo Mercury orbiter, an ESA Cornerstone mission.

2 Theoretical framework

An interesting generalization of GR includes a non-vanishing torsion. A class of theories allowing the presence of torsion is based on the extension of Riemann spacetime to Riemann-Cartan spacetime. The latter has a richer geometric structure, since it is endowed with a metric $g_{\mu\nu}$ and a connection $\Gamma^{\lambda}_{\ \mu\nu}$ which is not the Levi-Civita connection. A compatibility condition between $g_{\mu\nu}$ and $\Gamma^{\lambda}_{\ \mu\nu}$ is required, namely the covariant derivative of the metric tensor must vanish identically. Under this assumption the resulting connection turns out to be non-symmetric, and such a lack of symmetry gives origin to a non-vanishing torsion tensor. We refer to [14], [15] for the details.
In most torsion theories of gravity, the source of torsion is the intrinsic spin of matter [14], [16], [17]. A recent review on searches for the role of spin and polarization in gravity can be found in [18]. Since the spins of elementary particles in macroscopic matter are usually oriented in a random way, such theories predict a negligible amount of torsion generated by massive bodies. As a consequence spacetime torsion would be observationally negligible in the solar system.
However, in [19] Mao, Tegmark, Guth and Cabi (MTGC) argue that, if there are theories giving rise to detectable torsion in the solar system, they should be tested experimentally. For this reason, in [19] a theory-independent framework based on symmetry arguments is developed, and it is determined by a set of parameters describing the torsion and the metric. Here, by theory-independent framework, we mean the following: the metric and the connection are parametrized, around a massive body, with the help of symmetry arguments, without reference to a torsion model based on a specific Lagrangian (or even on specific field equations).
This framework can be used to constrain the above mentioned parameters from solar system experiments. In particular, MTGC suggest that GPB is an appropriate experiment for this task. In [19] the authors compute the precession of gyroscopes and find the constraints that GPB is able to place on the torsion parameters. In [20] Hehl and Obukhov argue that measuring torsion requires intrinsic spin, and criticize the approach of MTGC, since GPB gyroscopes do not carry uncompensated elementary particle spin.
MTGC address also the question whether there exists a specific gravitational Lagrangian which yields a torsion signal detectable by the GPB experiment. As an example they quote the theory by Hayashi and Shirafuji (HS) in [21] where a massive body generates a torsion field. In such a theory gravitational forces are due entirely to spacetime torsion and not to curvature. The same property is shared by teleparallel theories [22], [23], [24], [25], [26].
Then MTGC propose what they call the Einstein-Hayashi-Shirafuji (EHS) Lagrangian, which is a linear interpolation of GR and HS Lagrangians. The main feature of the EHS theory is that it admits both curvature and torsion.
The EHS model has been criticized by various authors. Flanagan and Rosenthal show in [27] that the linearized EHS theory becomes consistent only if the parameters in the Lagrangian satisfy suitable relations that, in turn, make the predictions coinciding with those of GR. In the paper [28], Puetzfeld and Obukhov derive the equations of motion in the framework of metric-affine gravity theories, which includes the HS theory, and show that only test bodies with microstructure (such as spin) can couple to torsion. The conclusion is that the EHS

theory does not yield a torsion signal detectable for GPB. For this reason, in [19] the EHS Lagrangian is proposed just as a pedagogical toy model. In the present paper we will not treat the EHS model.
As also remarked by Flanagan and Rosenthal in [27], the failure of constructing the specific EHS Lagrangian does not rule out the possibility that there may exist other torsion theories which could be usefully constrained by solar system experiments. Such torsion models should fit in the above mentioned theory-independent framework, similarly to a parametrized post-Newtonian framework including torsion. We remark that the parametrized formalism of MTGC does not take into account the intrinsic spin of matter as a possible source of torsion, and in this sense it cannot be a general torsion framework. However, it is adequate for the description of torsion around macroscopic massive bodies in the solar system, such as planets, being the intrinsic spin negligible when averaged over such bodies. For this reason we think it is worthwhile to continue the investigation of observable effects in the solar system of nonstandard torsion models within the MTGC parametrized formalism, under suitable working assumptions. In particular, our aim is to extend the GPB gyroscopes computations made in [19] to the case of motion of planets and satellites.
In the present paper we compute, as an effect of spacetime torsion, the corrections both to the precession of the pericenter of a body orbiting around a central mass, and to the orbital geodetic precession. We describe the torsion by means of three parameters t_1, t_2, t_3. Our computations show that a complete account of the precessions requires a parametrization of torsion up to an approximation order higher than the one considered in [19].
We consider the motion of a test body in a spherically symmetric field, and the motion of a satellite (either the Moon or LAGEOS) in the gravitational field of the Sun and the Earth. Since we use a parametrized framework without specifying the coupling of torsion to matter, we cannot derive the equations of motion of test bodies from the gravitational field equations. Therefore, in order to compute effects of torsion on the orbits of planets and satellites, we will work out the implications of the assumption that the trajectory of a test body is either an autoparallel curve or a geodesic. Such trajectories do not need to coincide when torsion is present. The computations will be carried out under the assumption of weak field and slow motion of the test body.
We will assume that the motion of the satellite is obtained by superimposing the fields of the Sun and the Earth, both computed as if these bodies were at rest. Observe that these assumptions are satisfied to a sufficient order of approximation in classical General Relativity.
As in the original paper of de Sitter [10], we characterize the motion using the orbital elements of the osculating ellipse. In terms of these orbital elements, the equations of motion then reduce to the Lagrangian planetary equations. We calculate the secular variations of the longitude Ω of the node and of the longitude $\widetilde{\omega}$ of the pericenter of the satellite. The computed secular variations show how the corrections to the orbital de Sitter effect depend on the torsion parameters t_1, t_2, t_3. In addition we calculate the secular variation of the longitude of the pericenter of a body orbiting around a central mass, and also in this case we find the corresponding dependence on t_1, t_2, t_3. The data from the LLR and MRR measurements are then used to constrain the relevant linear combinations of the torsion parameters.
Eventually, we consider the geodesic trajectories, and we find that torsion parameters cannot be constrained by solar system experiments.
The paper is organized as follows. In Section 3 we briefly recall the notion of spacetime with torsion. In Section 4 we recall from [19] how to parametrize the metric and torsion

tensors under the assumption of spherical symmetry, and we extend the parametrization up to a higher order of approximation. In Section 5 the connection up to the required order is given. In Section 6 we analyze the equations of autoparallel trajectories and we derive the related system of ordinary differential equations to second order. The expression of the system clearly reveals the perturbation due to torsion with respect to the de Sitter equations. In Section 7 we calculate the correction due to torsion to the precession of pericenter. In Section 8 we calculate the correction due to torsion of the third Kepler's law. In Section 9 we investigate the motion of a satellite in the gravitational field of the Sun and the Earth and we compute what we can call the perturbative forces due to torsion. In Section 10 we derive the time evolution of the orbital elements of the satellite, using the classical perturbation theory of Celestial Mechanics, particularly the Gauss form of the Lagrange planetary equations. In Section 11 we calculate the secular variations of the orbital elements of the satellite. In Section 12 we give multiplicative torsion biases relative to the GR predictions. In Section 13 we report the constraints on the parameters of our torsion model from LLR and MRR, which is one of the main goals of this paper. In Section 14 we analyze shortly the geodesic trajectories. In Section 15 we summarize the future prospects of the LLR and MRR measurements and we discuss the implications of proposed and approved space missions for the search reported in this paper. Eventually, in the Appendix we confirm using a different formalism the computation leading to (7.11), and we show that, in the autoparallel scheme, torsion produces an effect on the precession of pericenter which was not taken into account in [60].

3 Spacetime with torsion

We briefly recall the basic notions of Riemann-Cartan spacetimes [14], [15]. A spacetime equipped with a Lorentzian metric $g_{\mu\nu}$ and a connection $\Gamma^{\lambda}{}_{\mu\nu}$ compatible with the metric is called a Riemann-Cartan spacetime. Compatibility means that $\nabla_\mu g_{\nu\lambda} = 0$, where ∇ denotes the covariant derivative. We recall in particular that for any vector field v^λ

$$\nabla_\mu v^\lambda \equiv \partial_\mu v^\lambda + \Gamma^{\lambda}{}_{\mu\nu} v^\nu.$$

The connection is determined uniquely by $g_{\mu\nu}$ and by the torsion tensor

$$S_{\mu\nu}{}^{\lambda} \equiv \frac{1}{2}\left(\Gamma^{\lambda}{}_{\mu\nu} - \Gamma^{\lambda}{}_{\nu\mu}\right)$$

as follows:

$$\Gamma^{\lambda}{}_{\mu\nu} = \left\{ {\lambda \atop \mu\nu} \right\} - K_{\mu\nu}{}^{\lambda}, \tag{3.1}$$

where $\{\cdot\}$ is the Levi-Civita connection, and

$$K_{\mu\nu}{}^{\lambda} \equiv -S_{\mu\nu}{}^{\lambda} - S^{\lambda}{}_{\nu\mu} - S^{\lambda}{}_{\mu\nu} \tag{3.2}$$

is the contortion tensor. In the particular case when $\Gamma^{\lambda}{}_{\mu\nu}$ is symmetric with respect to μ, ν the torsion tensor vanishes. In the present paper we will consider the case of nonsymmetric connections $\Gamma^{\lambda}{}_{\mu\nu}$.
The Riemann tensor of the connection (3.1) is given by

$$R^{\lambda}{}_{\rho\nu\mu} = \partial_\nu \Gamma^{\lambda}{}_{\mu\rho} - \partial_\mu \Gamma^{\lambda}{}_{\nu\rho} + \Gamma^{\lambda}{}_{\nu\alpha}\Gamma^{\alpha}{}_{\mu\rho} - \Gamma^{\lambda}{}_{\mu\alpha}\Gamma^{\alpha}{}_{\nu\rho}. \tag{3.3}$$

The particular case of vanishing torsion tensor corresponds to Riemann spacetime of GR, while the particular case of vanishing Riemann tensor corresponds to the Weitzenböck space time [21].

4 Parametrizations of metric and torsion in spherical symmetry

Throughout this paper we use the natural gravitational units where $c = 1$ and $G = 1$. In the following we consider a spherically symmetric body of mass m. Introducing spherical coordinates (r, θ, ϕ), we parametrize the metric and torsion tensors in a region of space (out of the body) where the dimensionless quantity $\epsilon_m \equiv m/r << 1$ (i.e., r is large in comparison with the Schwarzschild radius of the body). As it will be shown in the sequel, such an approximation is accurate enough for the purpose of our computations[1].
We recall that Parametrized Post-Newtonian (PPN) calculations [29] show that a complete account of the pericenter precession must involve second order parameters in ϵ_m (for instance the PPN parameter β). Therefore, assuming spherical symmetry, we parametrize the metric tensor $g_{\mu\nu}$ to second order. Under the assumption of spherical symmetry the line element has the following general expression in spherical coordinates:

$$ds^2 = -h(r)dt^2 + f(r)dr^2 + \alpha(r)r^2[d\theta^2 + \sin^2\theta d\phi^2]. \tag{4.1}$$

We can choose $\alpha(r) = 1$, and to second order in m/r we have

$$h(r) = 1 + \mathcal{H}\frac{m}{r} + \mathcal{I}\frac{m^2}{r^2}, \qquad f(r) = 1 + \mathcal{F}\frac{m}{r} + \mathcal{L}\frac{m^2}{r^2}, \tag{4.2}$$

where $\mathcal{H}, \mathcal{F}, \mathcal{I}, \mathcal{L}$ are dimensionless parameters. The metric is then expressed in nonisotropic spherical coordinates. In the computations of trajectories that we will make in the following, only the function $h(r)$ is required to the second order in ϵ_m, while for $f(r)$ the first order approximation is sufficient.
We follow the notation of [19] for the parametrization of the metric tensor: the parametrization (4.2) reduces to the first order in ϵ_m to the one used in [19]. In the case of a PPN metric we have [30, Section 3.4.1]:

$$\mathcal{H} = -2, \qquad \mathcal{F} = 2\gamma, \qquad \mathcal{I} = 2(\beta - \gamma). \tag{4.3}$$

In the present paper all the others PPN parameters [29] are assumed to be negligible.
When spacetime torsion is present, our calculations show that a complete account of the precessions must involve a parametrization of the torsion tensor $S_{\mu\nu}{}^{\rho}$ up to second order in ϵ_m.
We now follow the spherical symmetry arguments used by [19]: to do this, it is convenient to parametrize the nonvanishing components of the torsion tensor in isotropic rectangular coordinates (t, x^1, x^2, x^3). We have

$$\begin{aligned} S_{0i}{}^{0} &= \mathcal{P}(r')\frac{x^i}{(r')^2}, \\ S_{jk}{}^{i} &= \mathcal{Q}(r')\frac{x^j\delta_{ki} - x^k\delta_{ji}}{(r')^2}, \end{aligned} \qquad i, j, k \in \{1, 2, 3\}, \tag{4.4}$$

where $r' = \sqrt{(x^1)^2 + (x^2)^2 + (x^3)^2}$, $\mathcal{P}(r'), \mathcal{Q}(r')$ are arbitrary dimensionless functions, and δ_{ij} is the Kronecker's symbol. If we consider such functions as depending on the dimensionless small quantity m/r', for the purposes of our computations (see Section 5) it is sufficient

[1] For example, considering the field of the Sun of mass m and the Earth and Mercury as test bodies at a distance r of the order of their orbit semi-major axes, one gets, respectively, $\epsilon_m \sim 2\times10^{-8}$ and $\epsilon_m \sim 5\times10^{-8}$.

to Taylor expand them up to the second order, hence we write

$$\mathcal{P}(r') = t_1 \frac{m}{2r'} + \widetilde{t}_3 \frac{m^2}{(r')^2}, \qquad \mathcal{Q}(r') = t_2 \frac{m}{2r'} + \widetilde{t}_4 \frac{m^2}{(r')^2}, \tag{4.5}$$

where $t_1, t_2, \widetilde{t}_3, \widetilde{t}_4$ are dimensionless constants. In the particular case of first order approximation, the above formulas yield the parametrization used in [19].
In order to transform (4.4) to nonisotropic spherical coordinates in which the metric (4.1) is expressed, it is convenient to first transform to isotropic spherical coordinates (r', θ, ϕ). We have for the non vanishing components of the torsion tensor

$$\begin{aligned} S_{tr'}{}^{t} =& t_1 \frac{m}{2(r')^2} + \widetilde{t}_3 \frac{m^2}{(r')^3}, \\ S_{r'\theta}{}^{\theta} =& S_{r'\phi}{}^{\phi} = t_2 \frac{m}{2(r')^2} + \widetilde{t}_4 \frac{m^2}{(r')^3}. \end{aligned} \tag{4.6}$$

We now further transform (4.6) to nonisotropic spherical coordinates. To the required second order of accuracy, the transformation takes the form $(t, r', \theta, \phi) \to (t, r, \theta, \phi)$ with $r \simeq r'(1 + \frac{\mathcal{F}}{2}\frac{m}{r'})$. The resulting expression of the components (4.6) of the torsion tensor in such coordinates is:

$$\begin{aligned} S_{tr}{}^{t} =& t_1 \frac{m}{2r^2} + t_3 \frac{m^2}{r^3}, \\ S_{r\theta}{}^{\theta} =& S_{r\phi}{}^{\phi} = t_2 \frac{m}{2r^2} + t_4 \frac{m^2}{r^3}. \end{aligned} \tag{4.7}$$

The constants t_3 and t_4 are related to t_1, t_2, $\widetilde{t}_3$ and $\widetilde{t}_4$ as follows:

$$t_3 = \widetilde{t}_3 - \frac{\mathcal{F}}{2} t_1, \qquad t_4 = \widetilde{t}_4 - \frac{\mathcal{F}}{2} t_2. \tag{4.8}$$

Therefore from (3.1) and (3.2) it follows that $\Gamma^{\lambda}_{\mu\nu}$ becomes an explicit function of t_1, t_2, t_3, t_4, and the remaining four parameters involved,

$$\Gamma^{\lambda}_{\mu\nu} = \Gamma^{\lambda}_{\mu\nu}\left(t_1, t_2, t_3, t_4, \mathcal{H}, \mathcal{F}, \mathcal{I}, \mathcal{L}, r, \theta, \phi\right).$$

Since the metric and the torsion are constructed so that the compatibility condition $\nabla_\mu g_{\lambda\nu} = 0$ is satisfied, then the metric parameters are independent of the torsion parameters.

5 The connection up to second order

Using (3.1) and (3.2), the nonvanishing components of the connection in spherical symmetry, approximated to second order in $\epsilon_m = m/r$, read as follows:

$$
\begin{aligned}
\Gamma^t{}_{tr} &= \left(t_1 - \frac{\mathcal{H}}{2}\right)\frac{m}{r^2} + \left(\frac{\mathcal{H}^2}{2} - \mathcal{I} + 2t_3\right)\frac{m^2}{r^3},\\
\Gamma^t{}_{rt} &= -\frac{\mathcal{H}m}{2r^2} + \left(\frac{\mathcal{H}^2}{2} - \mathcal{I}\right)\frac{m^2}{r^3},\\
\Gamma^r{}_{tt} &= \left(t_1 - \frac{\mathcal{H}}{2}\right)\frac{m}{r^2} + \left[\frac{\mathcal{H}\mathcal{F}}{2} - \mathcal{I} + t_1(\mathcal{H}-\mathcal{F}) + 2t_3\right]\frac{m^2}{r^3},\\
\Gamma^r{}_{rr} &= -\frac{\mathcal{F}m}{2r^2} + \left(\frac{\mathcal{F}^2}{2} - \mathcal{L}\right)\frac{m^2}{r^3},\\
\Gamma^r{}_{\theta\theta} &= -r + (\mathcal{F}+t_2)m - (\mathcal{F}^2 + t_2\mathcal{F} + \mathcal{L} - 2t_4)\frac{m^2}{r},\\
\Gamma^r{}_{\phi\phi} &= -r\sin^2\theta + (\mathcal{F}+t_2)\,m\sin^2\theta - \left(\mathcal{F}^2 + t_2\mathcal{F} + \mathcal{L} - 2t_4\right)\frac{m^2}{r}\sin^2\theta,\\
\Gamma^\theta{}_{r\theta} &= \Gamma^\phi{}_{r\phi} = \frac{1}{r},\\
\Gamma^\theta{}_{\theta r} &= \Gamma^\phi{}_{\phi r} = \frac{1}{r} - t_2\frac{m}{r^2} - 2t_4\frac{m^2}{r^3},\\
\Gamma^\theta{}_{\phi\phi} &= -\sin\theta\cos\theta,\\
\Gamma^\phi{}_{\theta\phi} &= \Gamma^\phi{}_{\phi\theta} = \frac{\cos\theta}{\sin\theta}.
\end{aligned}
$$

In the computations of trajectories that we will make in the sequel only the components $\Gamma^r{}_{tt}$ $\Gamma^t{}_{tr}$, $\Gamma^t{}_{rt}$ are required to the second order in ϵ_m, while for the remaining components the first order approximation is sufficient. The second order of approximation is used in Section 6 for $\Gamma^r{}_{tt}$, and in the Appendix for $\Gamma^t{}_{tr}$, $\Gamma^t{}_{rt}$. It follows that the parameters $\mathcal{L}$ and t_4 (differently from $\mathcal{I}$ and t_3) will not appear in the next sections, and consequently they will not be considered in the sequel of the paper.

6 Equations of autoparallel trajectories

The precise form of the equations of motion of bodies in the gravitational field depends on the way the matter couples to the metric and the torsion in the Lagrangian (or in the gravitational field equations). Here we consider the parametrized framework of Section 4 without specifying a coupling of torsion to matter, hence without specifying the field equations.

In a Riemann-Cartan spacetime there are two different classes of curves, autoparallel and geodesic curves, respectively, which reduce to the geodesics of Riemann spacetime when torsion is zero [14]. Autoparallels are curves along which the velocity vector is transported parallel to itself by the connection $\Gamma^\lambda{}_{\mu\nu}$. Geodesics are curves which are extremals of the length functional, and along which the velocity vector is transported parallel to itself by the Levi-Civita connection. In GR the two types of trajectories coincide while, in general, they may differ in the presence of torsion. They are identical when the torsion is totally skew-symmetric [14], a special condition which is not satisfied within our parametrization.

The equations of motion of bodies in the gravitational field follow from the field equations, as a consequence of the Bianchi identities. The method of Papapetrou [31] can be used to derive the equations of motion of a test body having internal structure, such as for instance a small extended object that may have either rotational angular momentum or net spin. In standard torsion theories the trajectories of test bodies with internal structure, in general, are neither autoparallels nor geodesics [14], [15], [32], while structureless test bodies, such as spinless test particles, follow geodesic trajectories.
In our computations of orbits of either a planet or a satellite (considered as a test body), we will neglect its internal structure. In a theory-independent framework we cannot derive the equations of motion from the gravitational field equations. Therefore we need some working assumptions on the trajectories of structureless test bodies: we will investigate the consequences of the assumption that the trajectories are either autoparallels or geodesics. Assuming the trajectory to be a geodesic is natural and consistent with standard torsion theories. However, we will see in Section 14 that the geodesics are the same as in the PPN framework. Hence new predictions related to torsion may arise only when considering the autoparallel trajectories, which will turn out to explicitely depend on torsion parameters. In the following we give some motivations which make worthwhile the investigation of autoparallel trajectories.
In the paper [33], Kleinert and Pelster argue that the closure failure of parallelograms in the presence of torsion adds an additional term to the geodesics which causes structureless test bodies to follow autoparallel trajectories. Kleinert et al. also argue in [33], [34] that autoparallel trajectories are consistent with the principle of inertia. Hehl and Obukhov in [20] criticized the approach of Kleinert et al., since the equations of autoparallel trajectories have not been derived from the energy-momentum conservation laws. Kleinert investigates this issue in [35] where the autoparallel trajectories are derived from the gravitational field equations via the Bianchi identities, in the case when torsion is derived from a scalar potential (see [15] for a discussion of such a kind of torsion).
In the papers [36], [37], using a reformulation of the theory of Brans-Dicke in terms of a connection with torsion [38], Dereli, Tucker et al. suggest that the autoparallel trajectory of a spinless test particle is a possibility that has to be taken into account. In [36] the results of the investigation of autoparallel trajectories are applied to the computation of the orbit of Mercury. In [39], [40] the equations of autoparallel trajectories are derived from the gravitational field equations and Bianchi identities, in the special case of matter modeled as a pressureless fluid, and torsion expressed solely in terms of the gradient of the Brans-Dicke scalar field.
The above mentioned results show that there is an interest in the autoparallels in spacetime with torsion, which make worthwhile their investigation in the present paper. The system of equations of autoparallel trajectories of a test body reads as

$$\frac{d^2x^\lambda}{d\tau^2} + \Gamma^\lambda{}_{\mu\nu}\frac{dx^\mu}{d\tau}\frac{dx^\nu}{d\tau} = 0, \tag{6.1}$$

where τ is the proper time [41]. Notice that only the symmetric part $\frac{1}{2}(\Gamma^\lambda{}_{\mu\nu} + \Gamma^\lambda{}_{\nu\mu})$ of the connection enters in (6.1); in addition, the totally antisymmetric part of $S_{\lambda\mu\nu}$ cannot be measured from (6.1).
The trajectory of a test body has to be a time-like curve. Since the connection is compatible with the metric the quantity $g_{\mu\nu}\frac{dx^\mu}{d\tau}\frac{dx^\nu}{d\tau}$ is conserved by parallel transport. The tangent vector $\frac{dx^\mu}{d\tau}$ to the trajectory undergoes parallel transport by the connection along the autoparallel. Therefore, an autoparallel that is time-like at one point has this same orientation

everywhere, so that the trajectory is strictly contained in the light cone determined by $g_{\mu\nu}$, in a neighbourhood of every of its points. Hence the compatibility of the connection with the metric ensures that autoparallels fulfil a necessary requirement for causality.
The equations (6.1) can be rewritten as

$$\frac{d^2x^\alpha}{dt^2} = -\left(\Gamma^\alpha_{\mu\nu} - \Gamma^0_{\mu\nu}\frac{dx^\alpha}{dt}\right)\frac{dx^\mu}{dt}\frac{dx^\nu}{dt} \tag{6.2}$$

for $\alpha \in \{1,2,3\}$. In our units $(\frac{dx^\alpha}{dt})^2$ and $\frac{d^2x^\alpha}{dt^2}$ are of the order of ϵ_m.
We use for x^α spherical coordinates (r,θ,ϕ). Substituting in (6.2) the expression of $\Gamma^\lambda_{\mu\nu}$ given in Section 5 one gets, to the order ϵ_m^2 of accuracy,

$$\begin{cases} \ddot{r} = -\dfrac{m}{r^2} + \mathcal{A}\dfrac{m}{r^2} + \mathcal{B}\dfrac{m^2}{r^3} + \mathcal{C}\dfrac{m}{r^2}\dot{r}^2 + (r+\mathcal{D}m)\,\dot{\theta}^2 + (r+\mathcal{D}m)\sin^2\theta\ \dot{\phi}^2, \\ \ddot{\theta} = \left(-\dfrac{2}{r} + \mathcal{E}\dfrac{m}{r^2}\right)\dot{r}\dot{\theta} + \sin\theta\cos\theta\ \dot{\phi}^2, \\ \ddot{\phi} = \left(-\dfrac{2}{r} + \mathcal{E}\dfrac{m}{r^2}\right)\dot{r}\dot{\phi} - 2\cot\theta\ \dot{\theta}\ \dot{\phi}, \end{cases} \tag{6.3}$$

where

$$\begin{cases} \mathcal{A} = -t_1 + \dfrac{\mathcal{H}}{2} + 1, \\ \mathcal{B} = -\dfrac{\mathcal{H}\mathcal{F}}{2} + \mathcal{I} - t_1(\mathcal{H}-\mathcal{F}) - 2t_3, \\ \mathcal{C} = t_1 - \mathcal{H} + \dfrac{\mathcal{F}}{2}, \\ \mathcal{D} = -\mathcal{F} - t_2. \\ \mathcal{E} = t_1 + t_2 - \mathcal{H}. \end{cases}$$

In order to take into account relativistic corrections, the right hand sides of (6.3) must be at least of second order in ϵ_m; this is guaranteed if Γ^r_{tt} is developed to second order in ϵ_m, while it is enough to develop the remaining components of the connection to the first order. System (6.3) to lowest order becomes

$$\frac{d\vec{v}}{dt} = -\left(t_1 - \frac{\mathcal{H}}{2}\right)\frac{m}{r^2}\hat{e}_r, \tag{6.4}$$

where $\hat{e}_r$ is the unit vector in the radial direction. Imposing the Newtonian limit it follows (see also [19, formula (23)])

$$t_1 - \frac{\mathcal{H}}{2} = 1, \tag{6.5}$$

hence $\mathcal{A} = 0$.

We now transform (6.3) in rectangular coordinates $x = r\sin\theta\cos\phi$, $y = r\sin\theta\sin\phi$, $z = r\cos\theta$. Writing x^1, x^2, x^3 for x, y, z we get

$$\begin{cases} \ddot{x}^\alpha = -m\dfrac{x^\alpha}{r^3} + \mathcal{B}m^2\ \dfrac{x^\alpha}{r^4} + \mathcal{E}m\dfrac{\dot{x}^\alpha\dot{r}}{r^2} + \mathcal{D}m\dfrac{x^\alpha}{r^3}\Phi^2 + \dfrac{3}{2}\mathcal{F}m\dfrac{x^\alpha}{r^3}\dot{r}^2, \qquad \alpha = 1,2,3, \\ \\ \Phi^2 \equiv \displaystyle\sum_{\alpha=1}^{3}(\dot{x}^\alpha)^2. \end{cases} \tag{6.6}$$

Note that in case of no torsion (i.e., $t_1 = t_2 = t_3 = 0$) and when $\mathcal{F} = 2$ and $\mathcal{I} = 0$ system (6.6) reduces to the equations of motion of General Relativity in the weak field approximation.

7 Precession of pericenter

From the second equation in (6.3) it follows that if θ and $\dot{\theta}$ vanish at one time then θ is identically zero. Therefore, assuming plane motion, the system (6.6) can be written in the form

$$\begin{cases} \ddot{x} = -\dfrac{m}{r^3}x + F_x, \\ \\ \ddot{y} = -\dfrac{m}{r^3}y + F_y, \end{cases}$$

where (F_x, F_y) is the perturbation with respect to the Newton force,

$$\begin{cases} F_x = \mathcal{B}m^2\dfrac{x}{r^4} + \mathcal{E}m\dfrac{\dot{x}\dot{r}}{r^2} + \mathcal{D}m\dfrac{x}{r^3}\Phi^2 + \dfrac{3}{2}\mathcal{F}m\dfrac{x}{r^3}\dot{r}^2, \\ \\ F_y = \mathcal{B}m^2\dfrac{y}{r^4} + \mathcal{E}m\dfrac{\dot{y}\dot{r}}{r^2} + \mathcal{D}m\dfrac{y}{r^3}\Phi^2 + \dfrac{3}{2}\mathcal{F}m\dfrac{y}{r^3}\dot{r}^2, \end{cases} \tag{7.1}$$

and now $\Phi^2 = \dot{x}^2 + \dot{y}^2$.
The vector (F_x, F_y) can be decomposed in the standard way along two mutually orthogonal axes as

$$\begin{cases} S = \dfrac{x}{r}F_x + \dfrac{y}{r}F_y, \\ \\ T = \dfrac{\partial(x/r)}{\partial u}F_x + \dfrac{\partial(y/r)}{\partial u}F_y. \end{cases} \tag{7.2}$$

Here S is the component along the instantaneous radius vector, T is the component perpendicular to the instantaneous radius vector in the direction of motion, where u is the argument of latitude. Then, substituting (7.1) into (7.2) gives

$$\begin{cases} S = \mathcal{B}\dfrac{m^2}{r^3} + \mathcal{C}m\dfrac{\dot{r}^2}{r^2} + \mathcal{D}m\dot{u}^2, \\ \\ T = \mathcal{E}m\dfrac{\dot{r}\dot{u}}{r}. \end{cases} \tag{7.3}$$

Let us now recall [42], [43] that, using the method of variation of constants,

$$r = \frac{a(1-e^2)}{1 + e\cos v}, \tag{7.4}$$

where a is the semimajor axis of the satellite orbit, e is the eccentricity, v is the true anomaly, and

$$\dot{r} = \frac{r^2 e \sin v}{a(1-e^2)}\dot{v}, \qquad r^2\dot{v} = na^2(1-e^2)^{1/2}, \tag{7.5}$$

$n = 2\pi/U$, U the period of revolution. Recall that, in the Newtonian approximation, $n^2 = m/a^3$ from the Kepler's third law. Following the standard astronomical notation, we let $\widetilde{\omega}$ be the longitude of the pericenter, and $u = v + \widetilde{\omega}$. We also recall the following planetary equation of Lagrange in the Gauss form [43, Ch. 6, Sec. 6]:

$$\frac{d\widetilde{\omega}}{dt} = \frac{(1-e^2)^{1/2}}{nae}\left[-S\cos v + T\left(1 + \frac{r}{a(1-e^2)}\right)\sin v\right]. \tag{7.6}$$

Notice that, since S and T are of the order ϵ_m^2, we have that $\frac{d\widetilde{\omega}}{dt}$ is of the order $\epsilon_m^{3/2}$. We are therefore allowed to make the approximation

$$\dot{u} \simeq \dot{v}. \tag{7.7}$$

Inserting (7.3) into (7.6), making also use of (7.4), (7.5), (7.7) and the Kepler's third law, we have

$$\frac{d\widetilde{\omega}}{dt} = -\frac{\mathcal{B}m^2}{n^2a^4e(1-e^2)}(1+e\cos v)\cos v\dot{v} - \frac{\mathcal{C}em}{a(1-e^2)}\sin^2 v\cos v\dot{v} \tag{7.8}$$

$$-\frac{\mathcal{D}m}{ae(1-e^2)}(1+e\cos v)^2\cos v\dot{v} + \frac{\mathcal{E}m}{a(1-e^2)}\sin^2 v(2+e\cos v)\dot{v}. \tag{7.9}$$

According to perturbation theory, we now regard the orbital elements on the right hand side of (7.8) as approximately constants. Therefore, integrating with respect to t, we obtain

$$\begin{aligned}\delta\widetilde{\omega} = &-\frac{\mathcal{B}m}{ae(1-e^2)}\left(\sin v + \frac{e}{2}v + \frac{e}{4}\sin(2v)\right)\\ &-\frac{\mathcal{C}em}{3a(1-e^2)}\sin^3 v - \frac{\mathcal{D}m}{ae(1-e^2)}\left(\sin v + ev + \frac{e}{2}\sin(2v) + e^2\sin v - \frac{e^2}{3}\sin^3 v\right)\\ &+\frac{\mathcal{E}m}{a(1-e^2)}\left(v - \frac{1}{2}\sin(2v) + \frac{e}{3}\sin^3 v\right).\end{aligned} \tag{7.10}$$

7.1 Correction to the precession of pericenter due to torsion

Secular terms appear in $\delta\widetilde{\omega}$. Using the expressions for $\mathcal{B}$, $\mathcal{D}$ and $\mathcal{E}$, such secular contributions are:

$$(\delta\widetilde{\omega})_{\text{sec}} = \left(-\mathcal{H} + \frac{\mathcal{F}}{2} + 2t_2 + t_1^2 - \frac{\mathcal{I}}{2} + t_3\right)\frac{m}{a(1-e^2)}v. \tag{7.11}$$

If $t_1 = t_2 = t_3 = 0$, using (4.3) then we find

$$(\delta\widetilde{\omega})_{\text{sec}} = (2 + 2\gamma - \beta)\frac{m}{a(1-e^2)}v, \tag{7.12}$$

which gives the precession of pericenter in terms of PPN parameters, as it can be found in [29, Chapter 7, formula (7.54)]. Moreover, when $\mathcal{H} = -2$, $\mathcal{F} = 2$ and $\mathcal{I} = 0$ (i.e., $\beta = \gamma = 1$) we find the usual expression of $(\delta\widetilde{\omega})_{\text{sec}}^{\text{GR}}$ given by General Relativity. In the case of Mercury, such a precession amounts to 42.98 arcsec/century.

Our formula for $\delta\widetilde{\omega}_{\rm sec}$ differs from the formula

$$(\delta\widetilde{\omega})_{\rm sec} = \frac{\mathcal{F}}{2}(\delta\widetilde{\omega})^{\rm GR}_{\rm sec}, \tag{7.13}$$

found by Mao et al. in [19, formula (C10)]. Formula (7.13) does not reproduce the PPN result (7.12) when the torsion parameters vanish, though it reproduces the GR result in the particular case $\mathcal{H} = -2$ and $\mathcal{F} = 2$. In the Appendix we compute the precession of pericenter following the method used in [19], obtaining again expression (7.11).
The precession of the pericenter in a reformulation of the Brans-Dicke theory in terms of a connection with torsion has also been computed in [36] by using autoparallel trajectories.

8 Correction to Kepler's third law

In this section we compute the relativistic correction of Kepler's third law for Earth motion, in the presence of torsion. This result will be used in the sequel, for the computation of the satellite geodetic precession. We note that such a correction was not necessary in the previous computation of the precession of pericenter at the required order of accuracy.
We introduce the following coordinates. We take a system of rectangular coordinates centered at the Sun. The triplet (ξ, η, ζ) denotes the Earth's coordinates in this system, and we assume that the ecliptic plane coincides with the plane $\zeta = 0$; we assume that the eccentricity is zero, so that the Earth's orbit is given by

$$\xi = \rho\cos L, \quad \eta = \rho\sin L, \quad \zeta = 0,$$

where ρ and L denote the radius of the orbit and the longitude of the Earth, respectively. Therefore, system (6.3), using $\theta = \pi/2$ and $\dot{\rho} = 0$, yields

$$-\frac{m}{\rho^2} + \mathcal{B}\frac{m^2}{\rho^3} + (\rho + \mathcal{D}m)\,\dot{L}^2 = 0, \tag{8.1}$$

where m, here and in the sequel, denotes the mass of the Sun, supposed spherically symmetric. It follows that $\dot{L} = \nu_0$, where ν_0 is constant, and that

$$\frac{m}{\rho^3} = \nu_0^2\frac{1-(\mathcal{F}+t_2)\,\frac{m}{\rho}}{t_1 - \frac{\mathcal{H}}{2} - \mathcal{B}\frac{m}{\rho}} = \nu_0^2\frac{1-(\mathcal{F}+t_2)\,\frac{m}{\rho}}{1-\mathcal{B}\frac{m}{\rho}}, \tag{8.2}$$

where we have used the Newtonian limit condition (6.5). Since the semi-major axis of the Earth's orbit is large with respect to the Schwarzschild radius of the Sun, we have $m/\rho \sim 2\times 10^{-8} << 1$. Since in our units $c = 1$, we also have that $\nu_0^2 << 1$. It follows that, up to second order, equation (8.2) becomes

$$\frac{m}{\rho^3} = \frac{\nu_0^2}{t_1 - \frac{\mathcal{H}}{2}}\left[1 - \frac{(t_1 - \frac{\mathcal{H}}{2})(\mathcal{F}+t_2) - \mathcal{B}}{t_1 - \frac{\mathcal{H}}{2}}\frac{m}{\rho}\right] = \nu_0^2\left[1 - (\mathcal{F}+t_2-\mathcal{B})\,\frac{m}{\rho}\right]. \tag{8.3}$$

This approximation will be used for the computation of the satellite geodetic precession in the next section.

9 Motion of a satellite in the field of the Sun and the Earth

In this section we investigate the motion of a satellite (either the Moon or LAGEOS) in the gravitational field of the Sun and the Earth in presence of torsion. The coordinates (ξ, η, ζ) have been defined in Section 8. The triplet (X, Y, Z) denotes the satellite's coordinates, and we set

$$\Delta^2 \equiv X^2 + Y^2 + Z^2.$$

The satellite's coordinates with respect to the Sun will be written as

$$X = \xi + x, \quad Y = \eta + y, \quad Z = \zeta + z,$$

where (x, y, z) are the coordinates of the satellite with respect to the Earth. We use the standard coordinates transformation [42], [43] used in Celestial Mechanics

$$\begin{cases} x = r(\cos u \cos \Omega - \sin u \sin \Omega \cos i), \\ \\ y = r(\cos u \sin \Omega + \sin u \cos \Omega \cos i), \\ \\ z = r \sin u \sin i, \end{cases} \tag{9.1}$$

where r is the distance between the Earth and the satellite, u is the argument of the latitude, Ω is the longitude of the node, and i is the orbital inclination.
We suppose that the Earth is spherically symmetric. The semi-major axes of the Moon and LAGEOS orbits around the Earth are small in comparison with ρ, so that in our computations we will neglect the powers of r/ρ greater than one[2]. Hence, also $m/\Delta << 1$. We will assume that the motion of the satellite is obtained by superimposing the fields (i.e., the connections as described in Section 5) of the Sun and the Earth, both computed as if these bodies were at rest. More precisely we assume

$$g_{\mu\nu} = (g_{\mu\nu})_0 + (g_{\mu\nu})_1^0 \qquad\qquad S_{\mu\nu}{}^{\lambda} = (S_{\mu\nu}{}^{\lambda})_0 + (S_{\mu\nu}{}^{\lambda})_1^0, \tag{9.2}$$

where

- $(g_{\mu\nu})_0$ and $(S_{\mu\nu}{}^{\lambda})_0$ are the metric and the torsion tensors, as given in Section 4, taking into account the Sun only, supposed at rest;
- $(g_{\mu\nu})_1^0$ and $(S_{\mu\nu}{}^{\lambda})_1^0$ are the metric and the torsion tensors taking into account the Earth only; these tensors are given at each time by the expressions in Section 4, computed as if the Earth were at rest (at that time).

Observe that these assumptions are satisfied to a sufficient order of approximation in classical General Relativity [10], [44] if all the terms that give rise to periodic perturbations are neglected (we are interested only in secular effects). We also note that a rigorous justification of the validity of (9.2) would probably require an extension of the parametrized torsion model to the case of three interacting bodies, which is beyond the scope of the present paper.
As a consequence we have

$$\frac{d^2x^\alpha}{dt^2} = \left(\frac{d^2x^\alpha}{dt^2}\right)_1^0 + \left(\frac{d^2X^\alpha}{dt^2}\right)_0 - \left(\frac{d^2\xi^\alpha}{dt^2}\right)_0,$$

where we write x^1, x^2, x^3 for x, y, z. Similarly we write X^1, X^2, X^3 for X, Y, Z, and ξ^1, ξ^2, ξ^3 for ξ, η, ζ. Moreover

[2]For the Moon and LAGEOS we have $r/\rho \sim 2.6 \times 10^{-3}$ and $r/\rho \sim 8.5 \times 10^{-3}$ respectively.

- $\left(\frac{d^2x^\alpha}{dt^2}\right)_1^0$ is the left hand side of (6.2) with the coefficients of the connection computed using $(g_{\mu\nu})_1^0$ and $(S_{\mu\nu}{}^\lambda)_1^0$;

- $\left(\frac{d^2X^\alpha}{dt^2}\right)_0$ is the left hand side of (6.2) with the coefficients computed using $(g_{\mu\nu})_0$ and $(S_{\mu\nu}{}^\lambda)_0$;

- $\left(\frac{d^2\xi^\alpha}{dt^2}\right)_0$ is the left hand side of (6.2) with the coefficients computed using $(g_{\mu\nu})_0$ and $(S_{\mu\nu}{}^\lambda)_0$.

The contribution of the term $\left(\frac{d^2x^\alpha}{dt^2}\right)_1^0$ gives a secular precession of the perigee which has been computed in Section 7. The other terms represent the perturbing effect of the Sun. Since all the perturbations here considered are small enough to allow us to superimpose them linearly, in what follows we compute the perturbing effect of the Sun only. With these assumptions, using the Newtonian limit (6.5) the right hand members of (6.6) give

$$\ddot{x}^\alpha + R^\alpha = k_A A^\alpha + k_B B^\alpha + k_C C^\alpha + k_D D^\alpha \quad \text{for } \alpha = 1, 2, 3, \tag{9.3}$$

where

$$\begin{cases} R^\alpha = m\left(\dfrac{X^\alpha}{\Delta^3} - \dfrac{\xi^\alpha}{\rho^3}\right), \\ A^\alpha = m^2\left(\dfrac{X^\alpha}{\Delta^4} - \dfrac{\xi^\alpha}{\rho^4}\right), \\ B^\alpha = m\left(\dfrac{\dot\Delta \dot X^\alpha}{\Delta^2} - \dfrac{\dot\rho\dot\xi^\alpha}{\rho^2}\right), \\ C^\alpha = m\left(\dfrac{X^\alpha \sum_\sigma (\dot X^\sigma)^2}{\Delta^3} - \dfrac{\xi^\alpha \sum_\sigma (\dot\xi^\sigma)^2}{\rho^3}\right), \\ D^\alpha = m\left(\dfrac{X^\alpha \dot\Delta^2}{\Delta^3} - \dfrac{\xi^\alpha \dot\rho^2}{\rho^3}\right), \end{cases}$$

and for notational convenience we set

$$k_A = \mathcal{B}, \quad k_B = \mathcal{E}, \quad k_C = \mathcal{D}, \quad k_D = \frac{3\mathcal{F}}{2}. \tag{9.4}$$

The left hand side of (9.3) contains the ordinary Newtonian perturbing function N^α, which also requires a correction $\widehat{N}^\alpha$, according to the computations in Section 8. This will be made clear in Section 10.
The components R^α and A^α, approximated to the first order with respect[3] to r/ρ and $\dot r/\rho$, read as follows (where we write R_x, R_y and R_z for R^1, R^2 and R^3 respectively, and similarly

[3]From formula (10.10) below expressing $\dot r$, it follows $|\dot r| \le \frac{r|\dot v|}{1-e}$, so that $\dot r$ is at least small as $\dot v$, hence $|\dot r/\rho|$ is smaller than r/ρ.

for A, B etc.):

$$\begin{cases} R_x = \dfrac{m}{\rho^3}\left(x - 3x\cos^2 L\right) + P_{R_x}, \\ R_y = \dfrac{m}{\rho^3}\left(y - 3y\sin^2 L\right) + P_{R_y}, \\ R_z = \dfrac{m}{\rho^3} z + P_{R_z}, \end{cases} \tag{9.5}$$

$$\begin{cases} A_x = \dfrac{m^2}{\rho^4}\left(x - 4x\cos^2 L\right) + P_{A_x}, \\ A_y = \dfrac{m^2}{\rho^4}\left(y - 4y\sin^2 L\right) + P_{A_y}, \\ A_z = \dfrac{m^2}{\rho^4} z + P_{A_z}. \end{cases} \tag{9.6}$$

Here the terms P_{R^α}, P_{A^α} denote a finite sum of addenda with the following property; each addendum is of the form $f\ (\sin L)^{n_1}(\cos L)^{n_2}$, where $n_1 + n_2$ is odd and f is a factor independent of L. Such terms will give periodic contributions to the perturbations of the orbital elements: therefore they will be neglected in the computation of secular perturbations.
The components B^α, C^α and D^α, approximated to the first order with respect to r/ρ, $\dot{r}/\rho$, and taking into account also the terms in $r\dot{r}/\rho^2$, read as follows:

$$\begin{cases} B_x = \dfrac{m\dot{L}}{\rho}(\dot{L}x - \dot{y})\sin^2 L + P_{B_x}, \\ B_y = \dfrac{m\dot{L}}{\rho}(\dot{L}y + \dot{x})\cos^2 L + P_{B_y}, \\ B_z = P_{B_z}, \end{cases} \tag{9.7}$$

$$\begin{cases} C_x = \dfrac{m\dot{L}}{\rho}\left(\dot{L}x + (-3\dot{L}x + 2\dot{y})\cos^2 L\right) + P_{C_x}, \\ C_y = \dfrac{m\dot{L}}{\rho}\left(\dot{L}y + (-3\dot{L}y - 2\dot{x})\sin^2 L\right) + P_{C_y}, \\ C_z = \dfrac{m\dot{L}^2}{\rho} z + P_{C_z}, \end{cases} \tag{9.8}$$

$$\begin{cases} D_x = P_{D_x}, \\ D_y = P_{D_y}, \\ D_z = P_{D_z}. \end{cases} \tag{9.9}$$

Also here the terms P_{B^α}, P_{C^α} and P_{D^α} have the same structure of P_{R^α} and P_{A^α}, thus giving periodic perturbations of the orbital elements.

10 Computation of orbital elements via perturbation theory

In this section we introduce the tools from Celestial Mechanics needed to compute the secular perturbations of the orbital elements. In the following the orbital elements, the true anomaly v and the argument of latitude u will be referred to the satellite's orbit around Earth.
Using the Newtonian limit condition (6.5) and the correction to Kepler's third law (8.3) we have

$$R^\alpha = N^\alpha - k_N \widehat{N}^\alpha \qquad \text{for } \alpha = 1,2,3, \tag{10.1}$$

where

$$\begin{cases} N_x = \nu_0^2 x\left(1 - 3\cos^2 L\right) + P_{N_x}, \\ N_y = \nu_0^2 y\left(1 - 3\cos^2 L\right) + P_{N_y}, \\ N_z = \nu_0^2 z + P_{N_z}, \end{cases} \tag{10.2}$$

$$\begin{cases} \widehat{N}_x = \dfrac{m\nu_0^2}{\rho} x(1 - 3\cos^2 L) + P_{\widehat{N}_x}, \\ \widehat{N}_y = \dfrac{m\nu_0^2}{\rho} y(1 - 3\sin^2 L) + P_{\widehat{N}_y}, \\ \widehat{N}_z = -\dfrac{m\nu_0^2}{\rho} z + P_{\widehat{N}_z}, \end{cases} \tag{10.3}$$

and

$$k_N = \mathcal{F} + t_2 - k_A. \tag{10.4}$$

Again the terms P_{N^α} and $P_{\widehat{N}^\alpha}$ give periodic contributions to the perturbations of the orbital elements.
In equation (10.1) R^α is decomposed into the ordinary Newtonian perturbing function N^α plus a relativistic correction $-k_N\widehat{N}^\alpha$, which depends also on torsion.
Equations (9.3) can be rewritten as

$$\ddot{x}^\alpha + N^\alpha = F^\alpha \qquad \text{for } \alpha = 1,2,3, \tag{10.5}$$

where F^α is the perturbation with respect to the Newton force, and it is given by

$$F^\alpha = k_N\widehat{N}^\alpha + k_A A^\alpha + k_B B^\alpha + k_C C^\alpha + k_D D^\alpha.$$

Recalling also (9.1), the perturbation (F_x, F_y, F_z) can be decomposed in the standard way along three mutually orthogonal axes as

$$\begin{cases} S = \dfrac{x}{r}F_x + \dfrac{y}{r}F_y + \dfrac{z}{r}F_z, \\ T = \dfrac{\partial(x/r)}{\partial u}F_x + \dfrac{\partial(y/r)}{\partial u}F_y + \dfrac{\partial(z/r)}{\partial u}F_z, \\ \sin u\ W = \dfrac{\partial(x/r)}{\partial i}F_x + \dfrac{\partial(y/r)}{\partial i}F_y + \dfrac{\partial(z/r)}{\partial i}F_z. \end{cases} \tag{10.6}$$

Here S is the component along the instantaneous radius vector, T is the component perpendicular to the instantaneous radius vector in the direction of motion, and W is the

component normal to the osculating plane of the orbit (collinear with the angular momentum vector).
Recalling from Section 8 that $\dot{L} = \nu_0$, $L = \nu_0 t$, we replace W, S, and T with the averages

$$\frac{\nu_0}{2\pi}\int_0^{2\pi/\nu_0} W\,dt, \qquad \frac{\nu_0}{2\pi}\int_0^{2\pi/\nu_0} S\,dt, \qquad \frac{\nu_0}{2\pi}\int_0^{2\pi/\nu_0} T\,dt,$$

respectively. Taking these averages has the following consequences: (i) it eliminates the dependence of W on the trigonometric functions of L, hence the periodic terms in (9.5)-(9.9) disappear; (ii) the remaining terms, contributing to the secular effects, are multiplied by a factor depending on ν_0.
In order to compute the components S, T and W of the perturbation, using the method of variation of constants [42], [43] we write

$$\begin{cases} \dot{x} = \dot{r}(\cos u\cos\Omega - \sin u\sin\Omega\cos i) + r\dot{u}(-\sin u\cos\Omega - \cos u\sin\Omega\cos i), \\ \dot{y} = \dot{r}(\cos u\sin\Omega + \sin u\cos\Omega\cos i) + r\dot{u}(-\sin u\sin\Omega + \cos u\cos\Omega\cos i), \\ \dot{z} = \dot{r}\sin u\sin i + r\cos u\sin i, \end{cases}$$

in order to eliminate $\dot{x}^\alpha$.
We recall that $u = v + \widetilde{\omega} - \Omega$ (where $\widetilde{\omega}$ is the longitude of the pericenter), which allows to make again the approximation $\dot{u} = \dot{v}$, and we make use of the area law $x\dot{y} - y\dot{x} = r^2\dot{v}\cos i$ in order to simplify the computations.
We decompose

$$W = W_A + W_B + W_C + W_{\widehat{N}},$$

with obvious meaning of the notation.
We have

$$\begin{cases} W_A = 2k_A\dfrac{m^2}{\rho^4}z\cos i, \\ W_B = k_B\dfrac{m\nu_0}{2\rho}\left(-\nu_0 z\cos i + \dot{v}z - \dot{r}\cos u\sin i\right), \\ W_C = k_C\dfrac{m\nu_0}{\rho}\left(\dfrac{3}{2}\nu_0 z\cos i - \dot{v}z + \dot{r}\cos u\sin i\right), \\ W_{\widehat{N}} = k_N\dfrac{m\nu_0^2}{\rho}\dfrac{3}{2}z\cos i. \end{cases} \tag{10.7}$$

Rearranging terms it follows

$$\begin{aligned} W =& \frac{m\nu_0^2}{\rho}\left(2k_A - \frac{k_B}{2} + \frac{3k_C}{2} + \frac{3k_N}{2}\right)z\cos i \\ &+ \frac{m\nu_0\dot{v}}{\rho}\left(\frac{k_B}{2} - k_C\right)z + \frac{m\nu_0}{\rho}\left(-\frac{k_B}{2} + k_C\right)\dot{r}\cos u\sin i. \end{aligned}$$

When $\mathcal{H} = -2$, $\mathcal{F} = 2$ and $\mathcal{I} = 0$ (i.e., $\beta = \gamma = 1$) and $t_1 = t_2 = t_3 = 0$, we find

$$W_{\mathrm{GR}} = \frac{3m\nu_0}{\rho}z\dot{v} - \frac{3m\nu_0}{\rho}\dot{r}\cos u\sin i.$$

When the satellite is the Moon, we have $\dot{r}\sin i = O(ei)$ which is negligible. In this case W_{GR} corresponds to the formula found by de Sitter in [10, (95)].
Now we compute the Gaussian component S of the perturbation. Analogously we decompose

$$S = S_A + S_B + S_C + S_{\widehat{N}}.$$

We have

$$\begin{cases} S_A = -k_A \dfrac{m\nu_0^2}{r\rho}(r^2 - 2z^2), \\ S_B = k_B \dfrac{m\nu_0}{2r\rho}\left[r^2\left(\nu_0 - \dot{v}\cos i\right) - \nu_0 z^2\right], \\ S_C = k_C \dfrac{m\nu_0}{r\rho}\left[r^2\left(-\dfrac{\nu_0}{2} + \dot{v}\cos i\right) + \dfrac{3}{2}\nu_0 z^2\right], \\ S_{\widehat{N}} = k_N \dfrac{m\nu_0^2}{2r\rho}\left(-r^2 + 3z^2\right). \end{cases} \tag{10.8}$$

Rearranging terms it follows

$$\begin{aligned} S = &\frac{m\nu_0}{r\rho}\left[\left(-k_A + \frac{k_B}{2} - \frac{k_C}{2} - \frac{k_N}{2}\right)\nu_0 r^2 + \left(-\frac{k_B}{2} + k_C\right)\dot{v}r^2\cos i\right. \\ &\left. + \left(2k_A - \frac{k_B}{2} + \frac{3}{2}k_C + \frac{3}{2}k_N\right)\nu_0 z^2\right]. \end{aligned}$$

When $\mathcal{H} = -2$, $\mathcal{F} = 2$ and $\mathcal{I} = 0$ and $t_1 = t_2 = t_3 = 0$, we find

$$S_{\mathrm{GR}} = -3\frac{m\nu_0\dot{v}}{\rho} r\cos i.$$

When the satellite is the Moon if we approximate $\cos i \simeq 1$ then S_{GR} corresponds to the formula found in [10, (95)].
Similarly we decompose

$$T = T_A + T_B + T_C + T_{\widehat{N}}.$$

We have

$$\begin{cases} T_A = 2k_A \dfrac{m^2}{\rho^4} z\cos u\sin i, \\ T_B = k_B \dfrac{m\nu_0}{2\rho}\left(-\nu_0 z\cos u\sin i + \dot{r}\cos i\right), \\ T_C = k_C \dfrac{m\nu_0}{\rho}\left(\dfrac{3}{2}\nu_0 z\cos u\sin i - \dot{r}\cos i\right), \\ T_{\widehat{N}} = \dfrac{3}{2}k_N \dfrac{m\nu_0^2}{\rho} z\cos u\sin i. \end{cases} \tag{10.9}$$

Rearranging terms it follows

$$T = \frac{m\nu_0}{\rho}\left[\left(2k_A - \frac{k_B}{2} + \frac{3}{2}k_C + \frac{3}{2}k_N\right)\nu_0 z\cos u\sin i + \left(\frac{k_B}{2} - k_C\right)\dot{r}\cos i\right].$$

When $\mathcal{H} = -2$, $\mathcal{F} = 2$ and $\mathcal{I} = 0$ and $t_1 = t_2 = t_3 = 0$, we find

$$T_{\mathrm{GR}} = 3\frac{m\nu_0}{\rho}\dot{r}\cos i.$$

When the satellite is the Moon if we approximate $\cos i \simeq 1$ then T_{GR} corresponds to the formula found in [10, (95)].
As for the computation of the precession of pericenter in Section 7, we use the formulae

$$r = \frac{a(1-e^2)}{1 + e\cos v}, \qquad \dot{r} = \frac{ae(1-e^2)\dot{v}\sin v}{(1+e\cos v)^2}. \tag{10.10}$$

We also recall the following planetary equations of Lagrange in the Gauss form [43, Ch. 6, Sec. 6]:

$$\begin{aligned}\frac{d\Omega}{dt} =& \frac{1}{na^2(1-e^2)^{1/2}\sin i}\ Wr\sin u,\\ \frac{d\widetilde{\omega}}{dt} =& \frac{(1-e^2)^{1/2}}{nae}\left[-S\cos v + T\left(1+\frac{r}{a(1-e^2)}\right)\sin v\right] + 2\sin^2\frac{i}{2}\ \frac{d\Omega}{dt},\end{aligned} \tag{10.11}$$

where $n = 2\pi/U$, U the period of revolution of the satellite around Earth.
We make the computations up to the first order with respect to the eccentricity e, and we use the following formula for the true anomaly [43, formula (2.6.7)]

$$v(t) = n(t-\tau) + 2e\sin\left[n(t-\tau)\right] + O(e), \tag{10.12}$$

where τ is the satellite time of perigee passage.

11 Precession of orbital elements in the presence of torsion

Using the expressions of S, T and W computed in the previous section and integrating (10.11) we find secular terms in the expressions of $\delta\Omega$ and $\delta\widetilde{\omega}$. According to perturbation theory, we regard the orbital elements as approximately constant in the computation of such integrals. Since $u = v + \widetilde{\omega} - \Omega$, we can make use of the approximation $\dot{u} \simeq \dot{v}$. Moreover we use the formula $na^2(1-e^2)^{1/2} = r^2\dot{v}$, and (10.12).
Let us first consider the computations for the node Ω. Substituting the decomposition (10.7) of W into the expression of $\frac{d\Omega}{dt}$ in (10.11), one has to compute the following three types of integrals:

$$\mathrm{I} = \int \frac{zr\sin u}{na^2(1-e^2)^{1/2}}\ dt, \qquad \mathrm{II} = \int \frac{z\dot{v}r\sin u}{na^2(1-e^2)^{1/2}}\ dt, \qquad \mathrm{III} = \int \frac{r\dot{r}\sin u\cos u}{na^2(1-e^2)^{1/2}}\ dt.$$

The integrals I and II yield periodic terms plus the following secular contributions:

$$\mathrm{I}_{\mathrm{sec}} = \frac{\sin i}{n}\left(t - \frac{v}{2n}\right), \qquad \mathrm{II}_{\mathrm{sec}} = \sin i\frac{t}{2},$$

where t is time. The integral III yields only periodic terms.
In conclusion, it turns out that the secular contributions to the variation of the node Ω are:

$$(\delta\Omega)_{\mathrm{sec}} = \frac{m\nu_0^2}{\rho}\left(2k_A - \frac{k_B}{2} + \frac{3k_C}{2} + \frac{3k_N}{2}\right)\left(t - \frac{v}{2n}\right)\frac{\cos i}{n} + \frac{m\nu_0}{\rho}\left(\frac{k_B}{2} - k_C\right)\frac{t}{2}. \tag{11.1}$$

Since $v = nt +$ periodic terms in v, inserting (9.4) and (10.4) into (11.1) we obtain

$$\begin{aligned}(\delta\Omega)_{\mathrm{sec}} =& \frac{1}{2}\frac{m\nu_0}{\rho}\Bigg\{ -\frac{\mathcal{H}}{2} + \mathcal{F} + \frac{t_1}{2} + \frac{3t_2}{2}\\ &- \frac{\nu_0}{2n}\cos i\left[\frac{\mathcal{H}}{2}(\mathcal{H}+\mathcal{F}) - \mathcal{I} - t_1\mathcal{F} + t_1 + t_2 + 2t_3\right]\Bigg\}\ t.\end{aligned} \tag{11.2}$$

Using the Newtonian limit (6.5) and setting

$$C_1 \equiv 1 - \frac{\mathcal{H}}{2} + 2\mathcal{F} + 3t_2, \qquad C_2 \equiv 1 + \frac{\mathcal{H}}{2} + \frac{\mathcal{H}^2}{2} - \mathcal{F} - \mathcal{I} + t_2 + 2t_3, \tag{11.3}$$

we obtain

$$(\delta\Omega)_{\rm sec} = \frac{1}{4}\frac{m\nu_0}{\rho}\left(C_1 - C_2\frac{\nu_0}{n}\cos i\right)\ t. \tag{11.4}$$

When torsion is zero, that is $t_1 = t_2 = t_3 = 0$, if we let $\mathcal{F} = 2\gamma$, $\mathcal{I} = 2(\beta - \gamma)$ and $\mathcal{H} = -2$ (PPN formalism) we obtain

$$(\delta\Omega)_{\rm sec} = \frac{1}{2}\frac{m\nu_0}{\rho}\,(1+2\gamma)\,t - \frac{1}{2}\frac{m\nu_0}{\rho}\,(1-\beta)\,\frac{\nu_0}{n}\cos i\ t. \tag{11.5}$$

The first term on the right hand side of (11.5) determines the usual geodetic precession effect. The second term is consistent with the computations in [45, formula (48A)], when the satellite is the Moon, so that we can approximate $\cos i \simeq 1$.
Letting $\gamma = \beta = 1$ we find the usual formula of geodetic precession in General Relativity found by de Sitter (see [10, formula (97)]),

$$(\delta\Omega)^{\rm GR}_{\rm sec} = \frac{3m\nu_0}{2\rho}t.$$

We recall that when the satellite is the Moon, this precession amounts to 1.92 arcsec/century.
Now we consider the computations for the perigee. The contribution of the gaussian component S to the variation $\delta\widetilde{\omega}$ of the perigee is given by the integral

$$-\frac{(1-e^2)^{1/2}}{nae}\int S\cos v\ dt. \tag{11.6}$$

Substituting the decomposition (10.8) of S into the above integral, one has to compute the following three types of integrals:

$$\mathrm{I}^S = \int r\cos v\ dt, \qquad \mathrm{II}^S = \int r\dot{v}\cos v\ dt, \qquad \mathrm{III}^S = \int \frac{z^2}{r}\cos v\ dt.$$

We evaluate such integrals for small values of the eccentricity e and, taking into account that e appears at the denominator of (11.6), we expand the integral up to the second order in e. This is accomplished by expanding r in (10.10) with respect to e, and inserting (10.12) in the resulting expression. Then each of the integrands of I^S, II^S, III^S turns out to be a sum of products of simple trigonometric functions, from which secular terms and periodic terms can be separated. Such integrals then yield the following secular contributions:

$$\mathrm{I}^S_{\rm sec} = -\frac{3}{2}ae(1-e^2)t, \qquad \mathrm{II}^S_{\rm sec} = -\frac{1}{2}ae(1-e^2)v,$$

and

$$\mathrm{III}^S_{\rm sec} = -\frac{3}{8}ae(1-e^2)\sin^2 i\left[3\sin^2(\widetilde{\omega}-\Omega) + \cos^2(\widetilde{\omega}-\Omega)\right]t. \tag{11.7}$$

In order to evaluate the integral III^S, since $z = r\sin u\sin i$, we have made use of the relation $u = v + \widetilde{\omega} - \Omega$ to express the trigonometric functions of u.
The contribution of the gaussian component T to the variation $\delta\widetilde{\omega}$ of the perigee is given by the integral

$$\frac{(1-e^2)^{1/2}}{nae}\int T\left(1 + \frac{r}{a(1-e^2)}\right)\sin v\ dt.$$

Substituting the decomposition (10.9) of T into the above integral, one has to compute the following two types of integrals:

$$\mathrm{I}^T = \int\left(1+\frac{r}{a(1-e^2)}\right)z\cos u\sin v\ dt, \qquad \mathrm{II}^T = \int\left(1+\frac{r}{a(1-e^2)}\right)\dot{r}\sin v\ dt.$$

As in the previous case, we evaluate such integrals for small values of the eccentricity e. Moreover, we will use the expression in (10.10) for $\dot{r}$ and the relation $u = v + \widetilde{\omega} - \Omega$. Then each of the integrands of I^T, II^T turns out to be a sum of products of simple trigonometric functions, and we can extract the following secular contributions:

$$\begin{aligned}\mathrm{I}^T_{\mathrm{sec}} =& \frac{7}{8} ae(1-e^2)\sin i \left[\sin^2(\widetilde{\omega}-\Omega) - \cos^2(\widetilde{\omega}-\Omega)\right] t,\\ \mathrm{II}^T_{\mathrm{sec}} =& ae(1-e^2)v.\end{aligned}$$

In conclusion, the secular contribution to the variation of the perigee $\widetilde{\omega}$ is:

$$\begin{aligned}(\delta\widetilde{\omega})_{\mathrm{sec}} =& \frac{1}{2}\frac{m\nu_0}{\rho}\left(\frac{k_B}{2} - k_C\right) t + \frac{3}{2}\frac{m\nu_0^2}{n\rho}\left(-k_A + \frac{k_B}{2} - \frac{k_C}{2} - \frac{k_N}{2}\right) t\\ &+ \frac{1}{2}\frac{m\nu_0^2}{n\rho}\left[5\sin^2 i \sin^2(\widetilde{\omega}-\Omega) - (1-\cos i)\right]\left(2k_A - \frac{k_B}{2} + \frac{3}{2}k_C + \frac{3}{2}k_N\right) t.\end{aligned} \tag{11.8}$$

Inserting (9.4) and (10.4) into (11.8) we obtain

$$\begin{aligned}(\delta\widetilde{\omega})_{\mathrm{sec}} =& \frac{1}{2}\frac{m\nu_0}{\rho}\left(-\frac{\mathcal{H}}{2} + \mathcal{F} + \frac{t_1}{2} + \frac{3t_2}{2}\right) t + \frac{3}{4}\frac{m\nu_0^2}{n\rho}\left(-\mathcal{H} - \mathcal{F} - \mathcal{I} + t_1 + t_2 + 2t_3 + t_1\mathcal{H}\right) t\\ &- \frac{1}{4}\frac{m\nu_0^2}{n\rho}\left[5\sin^2 i \sin^2(\widetilde{\omega}-\Omega) - (1-\cos i)\right]\left(\frac{\mathcal{H}}{2}(\mathcal{H}+\mathcal{F}) - \mathcal{I} - t_1\mathcal{F} + t_1 + t_2 + 2t_3\right) t.\end{aligned}$$

Using (6.5) and (11.3) we get

$$(\delta\widetilde{\omega})_{\mathrm{sec}} = \frac{1}{4}\frac{m\nu_0}{\rho}\left\{C_1 + C_2\frac{\nu_0}{n}\left[4 - \cos i - 5\sin^2 i \sin^2(\widetilde{\omega}-\Omega)\right]\right\}\ t. \tag{11.9}$$

When torsion is zero, in the PPN formalism we obtain

$$\begin{aligned}(\delta\widetilde{\omega})_{\mathrm{sec}} =& \frac{1}{2}\frac{m\nu_0}{\rho}(1+2\gamma)\ t + \frac{3}{2}\frac{m\nu_0}{\rho}(1-\beta)\frac{\nu_0}{n}\ t\\ &- \frac{1}{2}\frac{m\nu_0^2}{n\rho}\left[5\sin^2 i \sin^2(\widetilde{\omega}-\Omega) - (1-\cos i)\right](1-\beta)t.\end{aligned} \tag{11.10}$$

The first term on the right hand side of (11.10) determines the usual geodetic precession effect. The second term is consistent with the computations in [45, formula (48A)], when the satellite is the Moon, so that we can approximate $\cos i \simeq 1$ (and the third term becomes negligible).
Letting $\gamma = \beta = 1$ we find $C_1 = 6$, $C_2 = 0$, hence the usual formula of geodetic precession in General Relativity found by de Sitter (see [10, formula (97)]),

$$(\delta\widetilde{\omega})^{\mathrm{GR}}_{\mathrm{sec}} = \frac{3m\nu_0}{2\rho}t.$$

Both in $(\delta\Omega)_{\mathrm{sec}}$ and in $(\delta\widetilde{\omega})_{\mathrm{sec}}$ there appears the term

$$\frac{1}{4}\frac{m\nu_0}{\rho}\left(1 - \frac{\mathcal{H}}{2} + 2\mathcal{F} + 3t_2\right) t,$$

which is independent of n and thus of the details of the satellite's motion. This term can therefore be interpreted as the geodetic precession effect when torsion is present.

12 Torsion biases

In this section, similarly to [19], we define multiplicative torsion biases relative to the GR predictions. These torsion biases will be used to put constraints on torsion parameters from solar system experiments.
For the case of precession of the satellite orbital elements we define

$$b_\Omega \equiv \frac{(\delta\Omega)_{\rm sec}}{(\delta\Omega)^{\rm GR}_{\rm sec}}, \qquad\qquad b_{\widetilde{\omega}} \equiv \frac{(\delta\widetilde{\omega})_{\rm sec}}{(\delta\widetilde{\omega})^{\rm GR}_{\rm sec}}. \tag{12.1}$$

From (11.4) and (11.9) it follows

$$\begin{aligned} b_\Omega =& \frac{1}{6}\left(C_1 - C_2\frac{\nu_0}{n}\cos i\right), \\ b_{\widetilde{\omega}} =& \frac{1}{6}\left\{C_1 + C_2\frac{\nu_0}{n}\left[4 - \cos i - 5\sin^2 i \sin^2(\widetilde{\omega}-\Omega)\right]\right\}, \end{aligned} \tag{12.2}$$

where the constants C_1 and C_2 are defined in (11.3).
For the purpose of comparison of solar system experiments with the predictions from the present torsion theory, we will assume that all metric parameters take the same form as in PPN formalism, according to (4.3). We have

$$\begin{cases} C_1 = 2 + 4\gamma + 3t_2, \\ C_2 = 2 - 2\beta + t_2 + 2t_3, \end{cases} \tag{12.3}$$

and from (12.2) we obtain

$$\begin{cases} b_\Omega = \dfrac{1}{3}(1+2\gamma) + \dfrac{t_2}{2} - \dfrac{\nu_0}{3n}\cos i\left(1 - \beta + \dfrac{t_2}{2} + t_3\right), \\ \\ b_{\widetilde{\omega}} = \dfrac{1}{3}(1+2\gamma) + \dfrac{t_2}{2} + \dfrac{\nu_0}{3n}\left[4 - \cos i - 5\sin^2 i\sin^2(\widetilde{\omega}-\Omega)\right]\left(1 - \beta + \dfrac{t_2}{2} + t_3\right). \end{cases} \tag{12.4}$$

Note that the torsion correction to the geodetic precession in (12.4) (namely the term $\frac{1}{3}(1+2\gamma) + \frac{t_2}{2}$) differs from the corresponding one found for gyroscopes in [19, formula (47)] by a numerical factor of order of unity.
When the satellite is the Moon, we have $\cos i = 1 + O(i^2)$, $\sin^2 i = O(i^2)$, and we may approximate

$$\begin{cases} b_\Omega = \dfrac{1}{3}(1+2\gamma) + \dfrac{t_2}{2} - \dfrac{\nu_0}{3n}\left(1 - \beta + \dfrac{t_2}{2} + t_3\right), \\ \\ b_{\widetilde{\omega}} = \dfrac{1}{3}(1+2\gamma) + \dfrac{t_2}{2} + \dfrac{\nu_0}{n}\left(1 - \beta + \dfrac{t_2}{2} + t_3\right). \end{cases} \tag{12.5}$$

Similarly, considering now $\delta\widetilde{\omega}$ as the precession of pericenter computed in Section 7, we have

$$B_{\widetilde{\omega}} \equiv \frac{(\delta\widetilde{\omega})_{\rm sec}}{(\delta\widetilde{\omega})^{\rm GR}_{\rm sec}} = \frac{1}{3}\left(1 + \frac{\mathcal{H}^2}{4} + \frac{\mathcal{F}}{2} - \frac{\mathcal{I}}{2} + 2t_2 + t_3\right). \tag{12.6}$$

In the case of a PPN metric we find

$$B_{\widetilde{\omega}} = \frac{1}{3}\left(2 + 2\gamma - \beta + 2t_2 + t_3\right). \tag{12.7}$$

13 Constraining torsion with the Moon and Mercury

Here we compare the predicted torsion biases to experimental measurements in order to set limits on the torsion parameters.
Recent limits on various components of the torsion tensor, obtained in a different torsion model based on the fact that background torsion may violate effective local Lorentz invariance, have been obtained in [46]. See also [47], where constraints on possible new spin-coupled interactions using a torsion pendulum are described.

13.1 Moon: geodetic precession

The GR test of the geodetic precession, evaluated with LLR data and expressed as a relative deviation from the value expected in GR, is $K_{gp} = -0.0019 \pm 0.0064$ [8]. In our torsion theory this is to be compared with the first two terms on the right hand side of equation (12.4):

$$| \widehat{b}_{\widetilde{\omega}} - 1| = |\frac{1}{3}(1+2\gamma) + \frac{t_2}{2} - 1| = |\frac{2}{3}(\gamma - 1) + \frac{t_2}{2}| < 0.0064, \tag{13.1}$$

where, taking into account the last sentence at the end of Section 11, we define

$$\widehat{b}_{\widetilde{\omega}} \equiv \frac{1}{3}(1+2\gamma) + \frac{t_2}{2}.$$

Using the Cassini measurement $\gamma - 1 = (2.1 \pm 2.3) \times 10^{-5}$, we can neglect this term compared to the experimental uncertainty on K_{gp} and get the following constraint on t_2:

$$2 \mid \widehat{b}_{\widetilde{\omega}} - 1| = |t_2| < 0.0128. \tag{13.2}$$

The meaning of the constraint on the torsion parameter t_2 is the following. Using the value $(\delta\widetilde{\omega})^{\rm GR}_{\rm sec} = 1.92$ arcsec/century for the geodetic precession of the Moon's orbit in GR, the geodetic precession in the presence of torsion is

$$(\delta\widetilde{\omega})_{\rm sec} = \left[1 + \frac{2}{3}(\gamma - 1) + \frac{t_2}{2}\right] 1.92 \quad \text{arcsec/century}.$$

If the parameter t_2 had a value larger than 0.0128, this would imply the precession of the Moon's perigee would be (neglecting the contribution of $\gamma - 1$)

$$(\delta\widetilde{\omega})_{\rm sec} > (1 + 0.0064)1.92 \quad \text{arcsec/century},$$

which would be inconsistent with LLR data. If $t_2 < -0.0128$ we would have an analogous inconsistency. To give the reader a further feeling of the effect of a nonzero value of t_2 in terms of orbit displacement, we provide the following, extreme example. The 1.92 arcsec/century precession amounts to a perigee displacement of about 3 meters per lunar orbit period (about 27 days). A value $t_2 = 1$ would imply (neglecting the contribution of $\gamma - 1$) a geodetic precession in the presence of torsion of about 4.5 meters/lunar orbit period.
The relentless accumulation of LLR data, the mm range accuracy of the APOLLO station, the start or restart of LLR operation of additional ILRS[4] stations (like MLRO, the Matera Laser Ranging Observatory in the south of Italy) will provide continuous further improvements of the K_{gp} test and therefore, of this limit on t_2. Future improvements are possible also with current data and stations, by further developing and refining the current orbital software packages.

[4]International Laser Ranging Service; see http://ilrs.gsfc.nasa.gov/.

13.2 Mercury: perihelion advance

The perihelion advance of Mercury has been measured with planetary radar ranging by Shapiro et al. in 1989 [3]. They found it to be consistent with its GR value with a relative standard error of 10^{-3}. In the PPN framework, this can be used to "infer that $\beta = 1$ to within a standard error of $\sigma(\beta) = 0.003$" (quoted from [3]).
According to our torsion model, in the case of the PPN metric with the torsion bias given by (12.7), we get for Mercury the one standard deviation limit:

$$\begin{aligned} |B_{\widetilde{\omega}} - 1| = \frac{1}{3}|2\gamma - \beta - 1 + 2t_2 + t_3| < 0.001, \\ |2\gamma - \beta - 1 + 2t_2 + t_3| < 0.003, \\ |(2\gamma - 2) + (1 - \beta) + 2t_2 + t_3| < 0.003. \end{aligned} \tag{13.3}$$

Using the Cassini measurement $\gamma - 1 = (2.1 \pm 2.3) \times 10^{-5}$, we can neglect this term compared to the experimental uncertainty on the perihelion advance and get the constraint:

$$|1 - \beta + 2t_2 + t_3| < 0.003. \tag{13.4}$$

The limits (13.2) and (13.4) on the values of t_2 and $(1 - \beta) + t_3$ are represented graphically in fig. 1.
Combining the LLR and MRR constraints one gets on t_3 the following limit:

$$|1 - \beta + t_3| < 0.0286. \tag{13.5}$$

If we assume the Nordtvedt effect [48], and that the Nordtvedt parameter $\eta_N = 4\beta - \gamma - 3$, then the measured value [8] is $\beta = 1 + (1.2 \pm 1.1) \times 10^{-4}$, which makes $\beta - 1$ negligible compared to the experimental uncertainty on the perihelion advance. The constraint then becomes:

$$|2t_2 + t_3| < 0.003. \tag{13.6}$$

In this latter case, combining the LLR and MRR constraints one gets on t_3 the following limit:

$$|t_3| < 0.0286. \tag{13.7}$$

The meaning of the constraints on the torsion parameter t_3 is the following. Using the value $(\delta\widetilde{\omega})^{\mathrm{GR}}_{\mathrm{sec}} = 42.98$ arcsec/century for the precession of Mercury's perihelion in GR, the precession of the perihelion in the presence of torsion is (neglecting the contribution of $\gamma - 1$):

$$(\delta\widetilde{\omega})_{\mathrm{sec}} = \left[1 + \frac{1}{3}(1 - \beta + 2t_2 + t_3)\right] 42.98 \quad \text{arcsec/century}.$$

If the linear combination $(1 - \beta + 2t_2 + t_3)$ had a value larger than 0.003, this would imply the precession of Mercury's perihelion would be

$$(\delta\widetilde{\omega})_{\mathrm{sec}} > (1 + 0.001)42.98 \quad \text{arcsec/century}, \tag{13.8}$$

which would be inconsistent with MRR data. If the parameter t_2 takes the lowest value consistent with LLR data, i.e., if $t_2 = -0.0128$, then a value of the parameter t_3 larger than $(0.0286 + \beta - 1)$ would imply the inconsistency (13.8) with MRR data. If $\beta - 1$ is

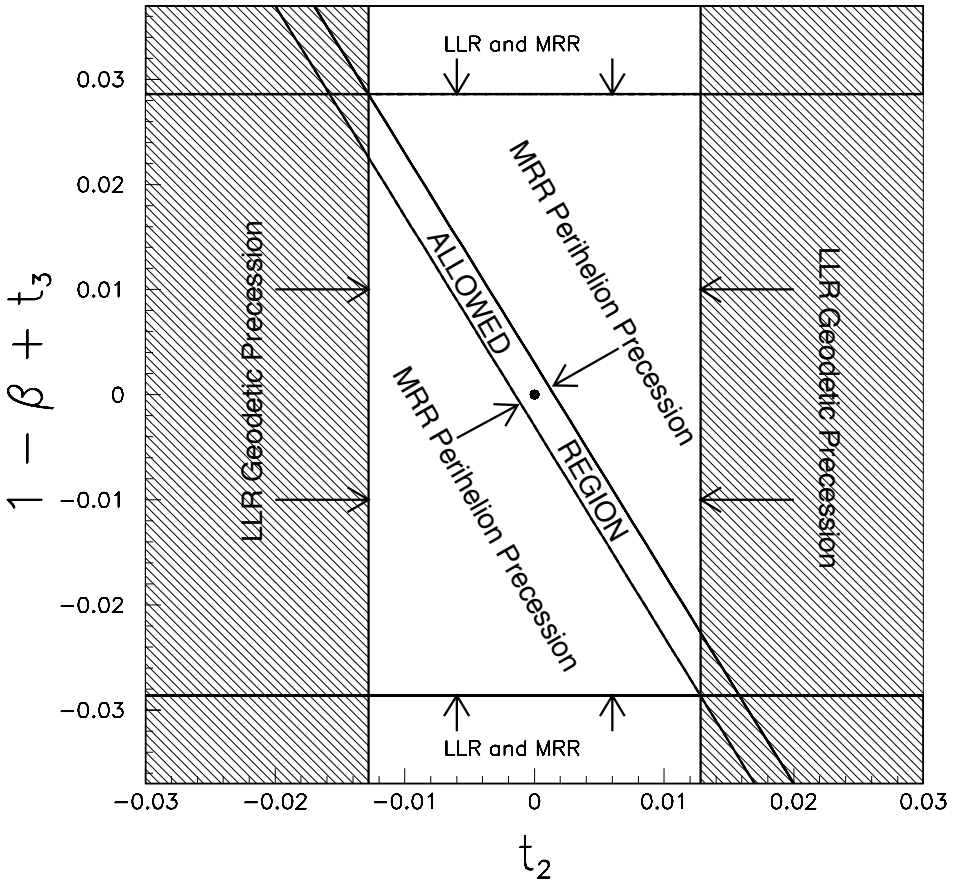

Figure 1: Constraints on t_2 and the linear combination $(1-\beta)+t_3$ from LLR and MRR, indicated by the arrows. For example, the hatched area is the region excluded by LLR only. General Relativity corresponds to $\beta - 1 = t_2 = t_3 = 0$ (black dot).

neglected, then simply $t_3 > 0.0286$ would be inconsistent with the data. Eventually, if $(1-\beta+2t_2+t_3) < -0.003$ we would have analogous inconsistencies.
We stress that the perihelion advance measurement used here is based on data taken between 1966 and 1990. As pointed out by Will ([1], page 38) "analysis of data taken since 1990 could improve the accuracy". Therefore, the above contraints on spacetime torsion can be improved already now, with existing data, while waiting that Mercury is reached by new spacecrafts, like in particular ESA's BepiColombo.

14 Equations of geodesics

In this section we consider the particular case of geodesic trajectories. The system of equations of geodesics trajectories reads as

$$\frac{d^2x^\lambda}{d\tau^2} + \left\{ \begin{matrix} \lambda \\ \mu\nu \end{matrix} \right\} \frac{dx^\mu}{d\tau} \frac{dx^\nu}{d\tau} = 0.$$

The resulting system of equations of motion is given by (6.3) with $t_1 = t_2 = t_3 = 0$. Such a system to lowest order becomes

$$\frac{d\vec{v}}{dt} = \frac{\mathcal{H}}{2} \frac{m}{r^2} \hat{e}_r.$$

Imposing the Newtonian limit (see also [19, formula (25)]) it follows that

$$\mathcal{H} = -2.$$

Hence all the precession formulae are the same as in the PPN formalism given in (7.12), (11.5) and (11.9). Therefore, if a satellite's orbit is assumed to be a geodesic, then the measurements of satellite experiments cannot be used to constrain the torsion parameters.

15 Discussion of the results and future prospects

This work is an investigation of the effects of spacetime torsion on the orbits of satellites and planets, based on a model with several parameters evolved from the one by MTGC. Due to the presence of a set of parameters, it must be tested with a combination of experiments designed to measure different physical effects and observables. In this case, no single experiment provides a complete answer, but experiments with the best accuracy and the broadest parameter sensitivity may find the first reliable hint of torsion. The notable example is the geodetic precession, which can be measured using three very different instrumental techniques: LLR, GPB's gyroscopes and future BepiColombo's radio science and accelerometer payloads. This makes constraining torsion with the geodetic precession robust against the effect of experimental systematic errors.
For completeness, we quote here that the constraints on torsion provided by the measurement of the geodetic precession turn out to be useful also in constraining spacetime torsion with the frame dragging experiments on LAGEOS satellites. We remark that the torsion corrections to the Lense-Thirring effect for LAGEOS and GPB contain different sets of torsion parameters. We refer to the companion paper [12] for the details.

15.1 Future prospects

Before the end of the decade, robotic missions on the lunar surface could deploy new scientific payloads which include laser retroreflectors and thus extend the LLR reach for new physics in three ways: (i) using a significantly improved 2^{nd} generation retroreflector design; (ii) increasing by a factor about 2 the geometric lever arm of LLR with missions to the lunar poles or limb; (iii) combining LLR payloads with transponders (at least two) for same-beam microwave interferometry (SBI) capable of additional accurate measurements of lunar rotations and librations [50], [51] (during the lifetime of the transponders).
In particular, the single, large, fused-silica retroreflector design developed by the University of Maryland and INFN-LNF [52] will improve over the performance of current Apollo arrays by a factor 100 or more, thus removing the dominant contribution to the LLR error budget.

Such a contribution is of the order of 2 cm. It is due to the multi-retroreflector structure of the arrays coupled to the librations and rotations of the Moon with respect to the Earth. The functionality of this specific new design, which inherits and is evolved from the successful Apollo 11, 14 and 15 experience, is being validated by thermal-vacuum-optical testing laboratory-simulated space conditions at the INFN-LNF "Satellite/lunar laser ranging Characterization Facility (SCF)" [53], [54], [55].
Other instruments, like the seismometer and the heat-flow probe, will provide important information to evaluate the LLR systematic errors related to the environmental conditions of the lunar surface and sub-surface layers of the lunar regolith.
After the end of this decade, results from the BepiColombo Mercury orbiter, an ESA Cornerstone mission equipped with a high-accuracy radio science and accelerometer payloads to test GR, is expected to improve the classical test of the perihelion advance [56], [57] (42.98 arcsec/century). The latter measurement can be cross-checked by new MRR data taken simultaneously with BepiColombo's ranging data (possibily, by the same ground stations). In addition, we note that in the past a Mercury orbiter like BepiColombo has been considered also for yet another independent measurement of the geodetic precession [58], [59] (20.50 arcsec/century; to be compared to the 1.92 arcsec/century for the Moon). Mercury's special role in the search for new physics effects, and for spacetime torsion in particular, is due to the relatively large value of its eccentricity and to its short distance to the Sun.
In conclusion, using current LLR and MRR data we have set constraints on the dimensionless torsion parameter t_2 and the linear combination $(1-\beta)+t_3$ at 10^{-2} level. In the future, LLR, MRR, GPB and, ultimately, BepiColombo together can exclude non-zero values of t_2 and t_3 with accuracies significantly below 1%.

16 Appendix

In this appendix we compute the precession of pericenter using the method in Appendix C of the online version [60].
The $\lambda = t$ component of (6.1) is

$$\frac{d^2t}{d\tau^2} + \left(\Gamma^t{}_{tr} + \Gamma^t{}_{rt}\right)\frac{dr}{d\tau}\frac{dt}{d\tau} = 0,$$

which yields

$$\frac{d^2t}{d\tau^2} + \left[t_1 - \mathcal{H} + \left(\mathcal{H}^2 - 2\mathcal{I} + 2t_3\right)\frac{m}{r}\right]\frac{m}{r^2}\frac{dr}{d\tau}\frac{dt}{d\tau} = 0,$$

from which one finds

$$\frac{d}{d\tau}\left[\exp\left(\int \psi(r)\ dr\right)\frac{dt}{d\tau}\right] = 0,$$

where

$$\psi(r) \equiv \left[t_1 - \mathcal{H} + \left(\mathcal{H}^2 - 2\mathcal{I} + 2t_3\right)\frac{m}{r}\right]\frac{m}{r^2}.$$

It follows the conservation law

$$k \equiv \exp\left\{-\left[t_1 - \mathcal{H} + \frac{1}{2}\left(\mathcal{H}^2 - 2\mathcal{I} + 2t_3\right)\frac{m}{r}\right]\frac{m}{r}\right\}\frac{dt}{d\tau} = \text{const.} \tag{16.1}$$

The $\lambda = \phi$ component of (6.1) when $\theta = \pi/2$ is

$$\frac{d^2\phi}{d\tau^2} + \left(\Gamma^\phi{}_{r\phi} + \Gamma^\phi{}_{\phi r}\right)\frac{dr}{d\tau}\frac{d\phi}{d\tau} = 0,$$

which yields

$$\frac{d^2\phi}{d\tau^2} + \left(\frac{2}{r} - t_2\frac{m}{r^2}\right)\frac{dr}{d\tau}\frac{d\phi}{d\tau} = 0,$$

where we can neglect the term with the factor $-2t_4\frac{m^2}{r^3}$. It follows the conservation law

$$h \equiv r^2\frac{d\phi}{d\tau}\exp\left(t_2\frac{m}{r}\right) = \text{const.} \tag{16.2}$$

Notice that k^2-1 and h^2 are of the order ϵ_m. Since the parameter τ is the proper time we have

$$\frac{ds^2}{d\tau^2} = g_{\mu\nu}\frac{dx^\mu}{d\tau}\frac{dx^\nu}{d\tau} = -1,$$

from which, for a test body in the equatorial plane $\theta = \pi/2$ it follows

$$-\left(1+\mathcal{H}\frac{m}{r}+\mathcal{I}\frac{m^2}{r^2}\right)\left(\frac{dt}{d\tau}\right)^2 + \left(1+\mathcal{F}\frac{m}{r}\right)\left(\frac{dr}{d\tau}\right)^2 + r^2\left(\frac{d\phi}{d\tau}\right)^2 = -1. \tag{16.3}$$

Observe that the term with the factor $\mathcal{I}$ is missing in [60, (C23)].
Using (16.1), (16.2) and the identity $dr/d\tau = (dr/d\phi)(d\phi/d\tau)$, from (16.3) it follows

$$\left(\frac{dr}{d\phi}\right)^2 = \frac{r^4\exp(2t_2\frac{m}{r})}{h^2\left(1+\mathcal{F}\frac{m}{r}\right)}\quad\left\{\quad -1+\frac{k^2\left(1+\mathcal{H}\frac{m}{r}+\mathcal{I}\frac{m^2}{r^2}\right)}{\exp\left\{-2\left[t_1-\mathcal{H}+\frac{1}{2}\left(\mathcal{H}^2-2\mathcal{I}+2t_3\right)\frac{m}{r}\right]\frac{m}{r}\right\}}\right.$$
$$\left. -\frac{h^2}{r^2\exp(2t_2\frac{m}{r})}\right\}. \tag{16.4}$$

We now need to expand the right hand side of (16.4) up to the order ϵ_m, since the left hand side is of order $O(1)$. The right hand side is divided by h^2, therefore we need to develop the quantity in $\{\cdots\}$ up to the order ϵ_m^2. Since k^2-1 is of the order ϵ_m, it is enough to develop the exponential in front of $\{\cdots\}$ up to the order ϵ_m. Taking into account that h^2 is of order ϵ_m, we have

$$\left(\frac{dr}{d\phi}\right)^2 = \frac{r^4}{h^2}\left[1+(2t_2-\mathcal{F})\frac{m}{r}\right]\quad\left\{\quad -1+k^2+k^2\left(2t_1-\mathcal{H}\right)\frac{m}{r}\right. \tag{16.5}$$
$$\left. +k^2\left[2t_1(t_1-\mathcal{H})+\mathcal{H}^2-\mathcal{I}+2t_3\right]\frac{m^2}{r^2}-\frac{h^2}{r^2}+2t_2h^2\frac{m}{r^3}\right\}.$$

From (16.5), setting $u \equiv 1/r$, we obtain the differential equation of the orbit

$$\frac{d^2u}{d\phi^2}+u = \frac{m}{2h^2}\left[k^2\left(-\mathcal{H}-\mathcal{F}+2t_1+2t_2\right)+\mathcal{F}-2t_2\right]+\frac{3}{2}\mathcal{F}mu^2+\frac{k^2}{h^2}Am^2u, \tag{16.6}$$

where

$$A \equiv \mathcal{H}\mathcal{F}+\mathcal{H}^2-\mathcal{I}-2t_1(\mathcal{H}+\mathcal{F})+2t_1^2+4t_1t_2-2t_2\mathcal{H}+2t_3, \tag{16.7}$$

where we have neglected the term containing u^3, which is of the order ϵ_m^2.
We stress that the term $\frac{k^2}{h^2}Am^2u$, neglected in the computations of [19], is of order ϵ_m, as well as the term $\frac{3}{2}\mathcal{F}mu^2$. Note also that $A=0$ in the case of GR, and that $A = 2(2-\gamma-\beta)$ in the case of PPN.

Using (6.5) and the above mentioned order of magnitude of k^2 it follows

$$\frac{d^2u}{d\phi^2} + \left(1 - \frac{A}{h^2}m^2\right) u = \frac{m}{h^2} + \frac{3}{2}\mathcal{F}mu^2. \tag{16.8}$$

In (16.8) we have neglected terms independent of u, originated by the expansion of k^2 inside $[\cdots]$ in (16.6), which have no effect on the precession of the pericenter.
If we neglect the last addendum on the right hand side of (16.8), and we set

$$c_1 \equiv \frac{m}{h^2}, \qquad \delta_1 \equiv \frac{3}{2}\mathcal{F}m, \qquad \delta_2 \equiv \frac{A}{h^2}m^2, \tag{16.9}$$

the solution u_0 of the corresponding linear equation is

$$u_0(\phi) = \frac{c_1}{1-\delta_2}\left\{1 + e\cos\left[\sqrt{1-\delta_2}\ (\phi - \phi_0)\right]\right\},$$

where e and ϕ_0 are constants of integration. If we neglect δ_2 with respect to 1, the above solution gives an elliptical orbit with eccentricity e and semi-latus rectum $p = a(1-e^2) = \frac{1-\delta_2}{c_1}$. Substituting u_0^2 in place of u^2 in (16.8), the solution u of the corresponding linearized equation is $u = u_0 + u_1$, where

$$\begin{aligned} u_1(\phi) =& \frac{\delta_1 c_1^2}{(1-\delta_2)^2}\Big[\frac{1+e^2/2}{1-\delta_2} + \frac{e}{\sqrt{1-\delta_2}}(\phi-\phi_0)\sin\left(\sqrt{1-\delta_2}\ (\phi-\phi_0)\right) \\ & - \frac{1}{1-\delta_2}\frac{e^2}{6}\cos\left(2\sqrt{1-\delta_2}\ (\phi-\phi_0)\right)\Big]. \end{aligned}$$

If the eccentricity of the orbit is small (i.e., $e^2 << e$) and we neglect the (small) additive constant $\frac{\delta_1 c_1^2}{(1-\delta_2)^2}\frac{1+e^2/2}{1-\delta_2}$ which does not contribute to the precession of the pericenter, we have

$$u(\phi) \simeq \frac{c_1}{1-\delta_2}\left\{1 + e\left[\cos\left(\sqrt{1-\delta_2}\ (\phi-\phi_0)\right) + \frac{c_1\delta_1}{(1-\delta_2)^{3/2}}(\phi-\phi_0)\sin\left(\sqrt{1-\delta_2}\ (\phi-\phi_0)\right)\right]\right\}.$$

Taking into account that $\frac{c_1\delta_1}{(1-\delta_2)^{3/2}}(\phi-\phi_0)$ is of order ϵ_m and that δ_2 is of order ϵ_m, we find

$$\begin{aligned} u(\phi) \quad & \simeq \frac{c_1}{1-\delta_2}\left[1 + e\cos\left(\phi - \phi_0 - c_1\delta_1(\phi-\phi_0) - \frac{\delta_2}{2}\left(1+3c_1\delta_1\right)(\phi-\phi_0)\right)\right] \\ & \simeq \frac{c_1}{1-\delta_2}\left\{1 + e\cos\left[(\phi-\phi_0)\left(1 - c_1\delta_1 - \frac{\delta_2}{2}\right)\right]\right\}. \end{aligned}$$

This is the equation of an elliptic orbit whose pericenter precedes according to

$$(\delta\widetilde{\omega})_{\rm sec} = 2\pi\left(\frac{1}{1 - c_1\delta_1 - \frac{\delta_2}{2}} - 1\right) \simeq 2\pi\left(c_1\delta_1 + \frac{\delta_2}{2}\right). \tag{16.10}$$

Substituting (16.7) and (16.9) into (16.10) we obtain formula (7.11).

17 Acknowledgements

We thank the University of Roma "Tor Vergata", CNR and INFN for supporting this work. We wish to thank B. Bertotti for some useful advices.

References

[1] C. M. Will, gr-qc/0510072.

[2] I.I. Shapiro, Rev. Mod. Phys. **71**, Centenary, S41 (1999).

[3] I.I. Shapiro, *Gravitation and Relativity 1989*, edited by N. Ashby, D.F. Bartlett, and W. Wyss, Cambridge University Press, Cambridge, England, 1990, p. 313.

[4] R. F. C. Vessot et al., Phys. Rev. Lett. **45**, 2081 (1980).

[5] S.S. Shapiro, J.L. Davis, D.E. Lebach, J.S. Gregory, Phys. Rev. Lett. **92**, 121101 (2004).

[6] R.D. Reasenberg et al., Astrophys. J. Lett. **234**, L219L221 (1979).

[7] B. Bertotti, L. Iess, P. Tortora, Nature **425**, 374 (2003).

[8] J. G. Williams, S. G. Turyshev, D. H. Boggs, Phys. Rev. Lett. **93**, 261101 (2004).

[9] I. Ciufolini, E.C. Pavlis, Nature **431**, 958 (2004).

[10] W. de Sitter, Monthly Notices of Royal Astr. Soc. **77** (Second Paper), 155 (1916).

[11] I.I. Shapiro, R.D. Reasenberg, J.F. Chandier, R.W. Babcock, Phys. Rev. Lett. **61**, 2643 (1988).

[12] R. March, G. Bellettini, R. Tauraso, S. Dell'Agnello, arXiv gr-qc/1101.2791.

[13] J. Battat et al., PASP **121**, 29 (2009).

[14] F.W. Hehl, P. von der Heyde, G.D. Kerlick, J.M. Nester, Rev. Mod. Phys. **48**, 393 (1976).

[15] R.T. Hammond, Rep. Prog. Phys. **65**, 599 (2002).

[16] W.R. Stoeger, P.B. Yasskin, Gen. Rel. Gravit. **11**, 427 (1979).

[17] P.B. Yasskin, W.R. Stoeger, Phys. Rev. D **21**, 2081 (1980).

[18] W-T Ni, Rep. Prog. Phys. **73**, 056901 (2010).

[19] Y. Mao, M. Tegmark, A.H. Guth, S. Cabi, Phys. Rev. D **76**, 1550 (2007).

[20] F.W. Hehl, Y.N. Obukhov, Annal. Fondation Louis de Broglie **32**, 157 (2007).

[21] K. Hayashi, T. Shirafuji, Phys. Rev. D **19**, 3524 (1979).

[22] W. Kopczynski, J. Phys. A: Math. Gen. **15**, 493 (1982).

[23] F. Mueller-Hoissen, J. Nitsch, Phys. Rev. D **18**, 718 (1983).

[24] J. Nester, Class. Quant. Grav. **5**, 1003 (1988).

[25] M. Blagojevich, I.A. Nikolic, Phys. Rev. D **62**, 024021 (2000).

[26] H.I. Arcos, J.G. Pereira, Int. J. Mod. Phys. D **13**, 2193 (2004).

[27] E.F. Flanagan, E. Rosenthal, Phys. Rev. D **75**, 124016 (2007).

[28] D. Puetzfeld, Y.N. Obukhov, Phys. Lett. A **372**, 6711 (2008).

[29] C.M. Will, *Theory and Experiment in Gravitational Physics*, Cambridge Univ. Press (1993).

[30] I. Ciufolini, J.A. Wheeler, *Gravitation and Inertia*, Princeton Univ. Press, Princeton (1995).

[31] A. Papapetrou, Proc. Roy. Soc. A **209**, 248 (1951).

[32] O.V. Babourova, B.N. Frolov, Phys. Rev. D **82**, 27503 (2010).

[33] H. Kleinert, A. Pelster, Gen. Rel. Grav. **31**, 1439 (1999).

[34] H. Kleinert, S.V. Shabanov, Phys. Lett. B **428**, 315 (1998).

[35] H. Kleinert, Gen. Rel. Grav. **32**, 769 (2000).

[36] T. Dereli, R.W. Tucker, Mod. Phys. Lett. A **17**, 421 (2002).

[37] H. Cebeci, T. Dereli, R.W. Tucker, Int. J. Mod. Phys. D **13**, 137 (2004).

[38] T. Dereli, R.W. Tucker, Phys. Lett. B **110**, 206 (1982).

[39] T. Dereli, R.W. Tucker, arXiv gr-qc/0107017.

[40] D.A. Burton, T. Dereli, R.W. Tucker, in *Symmetries in Gravity and Field Theory*, edited by V. Aldaya, J.M. Cerveró and Y.P. Garcia (Ediciones Universidad Salamanca, 2004), p. 237.

[41] V.N. Ponomariev, Bull. Acad. Polon. Sci. **XIX**, 6 (1971).

[42] D. Brouwer, G.M. Clemence, *Methods of Celestial Mechanics*, Academic Press (1961).

[43] F.T. Geyling, H.R. Westerman, *Introduction to Orbital Mechanics*, Addison Wesley (1971).

[44] W. de Sitter, KNAW, Proceedings, **19** I, Amsterdam, 367 (1917).

[45] A.M. Finkelstein, V. Ja. Kreinovich, Celestial Mech. **13**, 151 (1976).

[46] V.A. Kostelecky, N. Russell, J. Tasson, Phys. Rev. Lett. **100**, 111102 (2008).

[47] B.R. Heckel et al., Phys. Rev. D **78**, 092006 (2008).

[48] K. Nordtvedt, Jr., Phys. Rev. **169**, 1014 (1968); K. Nordtvedt, Jr., Phys. Rev. **169**, 1017 (1968); K. Nordtvedt, Jr., Phys. Rev. **170**, 1186 (1968).

[49] N. Toma, Progr. Theor. Phys. **86**, 659 (1991).

[50] M. Fermi et al. "37th COSPAR Scientific Assembly" (2008), July 13-20, Montréal, Canada, 868.

[51] P. L. Bender, Adv. Space Res. **14**, 233-242 (1994).

[52] D. G. Currie et al., "60th International Astronautical Congress", Daejeon, Korea, October 12-16, 2009, Paper n. IAC-09.A2.1.11.

[53] S. Dell'Agnello et al., in "Proceedings of the 16th International Workshop on Laser Ranging" (2008), October 13-17, Poznan, Poland, 121.

[54] S. Dell'Agnello et al., Adv. Space Res., *Galileo Special Issue*, **47** (2011) 822-842.

[55] S. Dell'Agnello et al., Exp. Astron., *MAGIA Special Issue*, DOI 10.1007/s10686-010-9195-0 (2010).

[56] A. Milani et al., Phys. Rev. D **66**, 082001 (2002).

[57] N. Ashby, P. L. Bender, J. M. Warh, Phys. Rev. D **75**, 022001 (2007).

[58] S. G. Turyshev, J. D. Anderson, R. W. Hellings, arXiv:gr-qc/9606028v1.

[59] J. D. Anderson et al., Planetary Space Sci. **45**, 21 (1997).

[60] Y. Mao, M. Tegmark, A.H. Guth, S. Cabi, arXiv:gr-qc/0608121v4.